AN ABSTRACT OF THE THESIS OF

JERRY LEE KRAUSE (Name) for the DOCTOR OF PHILOSOPHY (Degree)

in CHEMISTRY (Major) presented on July 25, 1969 (Date)

Title: AN INVESTIGATION OF THE SIMULTANEOUS DIFFUSION OF Pb^{++} AND Cd^{++} IN NaCl CRYSTALS AND KCl CRYSTALS

Abstract approved: Redacted for Privacy

William J. Fredericks

By a common ion treatment, the Stasiw-Teltow-Lidiard association theory was adapted to include the effect of two impurity ions on the equilibrium of the impurity-vacancy complex. A method of finite differences was adapted to solve two diffusion equations simultaneously when the diffusing species are the impurity-vacancy complexes.

Simultaneous diffusion of Pb^{++} and Cd^{++} in KCl crystals was studied. The saturation diffusion coefficient for the Pb^{++}-vacancy complex can be represented by

$$D_{s(Pb)} = 1.00 \times 10^{-3} \exp(-0.908 ev/kT) \text{ cm}^2/\text{sec}$$

and that for the Cd^{++}-vacancy complex by

$$D_{s(Cd)} = 4.05 \times 10^{-5} \exp(-0.557 ev/kT) \text{ cm}^2/\text{sec}.$$

The Gibbs free energy of association of the impurity-vacancy complex

in KCl for lead can be represented as

$$\Delta G_{Pb} = -0.378\text{ev} - (1.604 \times 10^{-4}\text{ev}/^{\circ}\text{K})\ T$$

and for cadmium as

$$\Delta G_{Cd} = -0.474\text{ev} - (1.230 \times 10^{-4}\text{ev}/^{\circ}\text{K})\ T.$$

Simultaneous diffusion of Pb^{++} and Cd^{++} in NaCl crystals was also studied. The saturation diffusion coefficient for the Pb^{++}-vacancy complex can be represented by

$$D_{s(Pb)} = 1.40 \times 10^{-2} \exp(-0.982\text{ev}/kT)\ \text{cm}^2/\text{sec}$$

and that for the Cd^{++}-vacancy complex by

$$D_{s(Cd)} = 3.57 \times 10^{-3} \exp(-0.857\text{ev}/kT)\ \text{cm}^2/\text{sec}.$$

The Gibbs free energy of association of the impurity-vacancy complex in NaCl for lead can be represented as

$$\Delta G_{Pb} = -0.775\text{ev} + (5.29 \times 10^{-4}\text{ev}/^{\circ}\text{K})\ T$$

and for cadmium as

$$\Delta G_{Cd} = -0.972\text{ev} + (6.65 \times 10^{-4}\text{ev}/^{\circ}\text{K})\ T.$$

An Investigation of the Simultaneous Diffusion of Pb^{++} and Cd^{++} in NaCl Crystals and KCl Crystals

by

Jerry Lee Krause

A THESIS

submitted to

Oregon State University

in partial fulfillment of
the requirements for the
degree of

Doctor of Philosophy

June 1970

APPROVED:

Redacted for Privacy

Professor of Chemistry
in charge of major

Redacted for Privacy

Chairman of the Department of Chemistry

Redacted for Privacy

Dean of Graduate School

Date thesis is presented July 25, 1969

Typed by Gwendolyn Hansen for Jerry Lee Krause

ACKNOWLEDGMENT

The author thanks Dr. W. J. Fredericks for suggesting the problem and for providing guidance and assistance throughout this work.

Thanks are especially due to David Hinks, Tony Allen and Al Propp for many useful suggestions and discussions, and double thanks to Al Propp for proofreading this thesis.

The author also expresses thanks to the Department of Health, Education and Welfare for financial assistance in the form of an NDEA fellowship, to the Shell Foundation for a teaching fellowship and to NSF for a research assistantship.

Finally, the author wishes to thank his parents, whose encouragement and help have made the completion of this thesis possible.

TABLE OF CONTENTS

LIST OF TABLES

LIST OF FIGURES

AN INVESTIGATION OF THE SIMULTANEOUS DIFFUSION OF Pb^{++} AND Cd^{++} IN NaCl CRYSTALS AND KCl CRYSTALS

I. INTRODUCTION

The process of diffusion has been used to study defects of the solid and the interactions of these defects. These studies have also provided information about the mechanisms of motion, such as the activation energy of migration.

The theories and studies of diffusion in ionic solids have been extensively discussed in several excellent books and review articles (17, p. 26-54, 82-104; 18, 19, p. 179-206; 25, 35, p. 137-151). Therefore, this introduction will only provide the language, theory, and background necessary for a development of the intended problem.

The structure of ionic solids can be thought to be a regular arrangement of positive and negative ions. In the case of NaCl or KCl, which are alkali halides having the NaCl structure, this structure is described by a face-centered cubic space lattice with a basis of one metal ion and one halide ion separated by one-half the body diagonal of the unit cube. The two-dimensional representation of the NaCl structure is very convenient to use, and the one shown in Figure (1.1) is used in future discussion.

Every lattice site in a perfect crystal would be occupied by the appropriate ion. However, the second law of thermodynamics implies

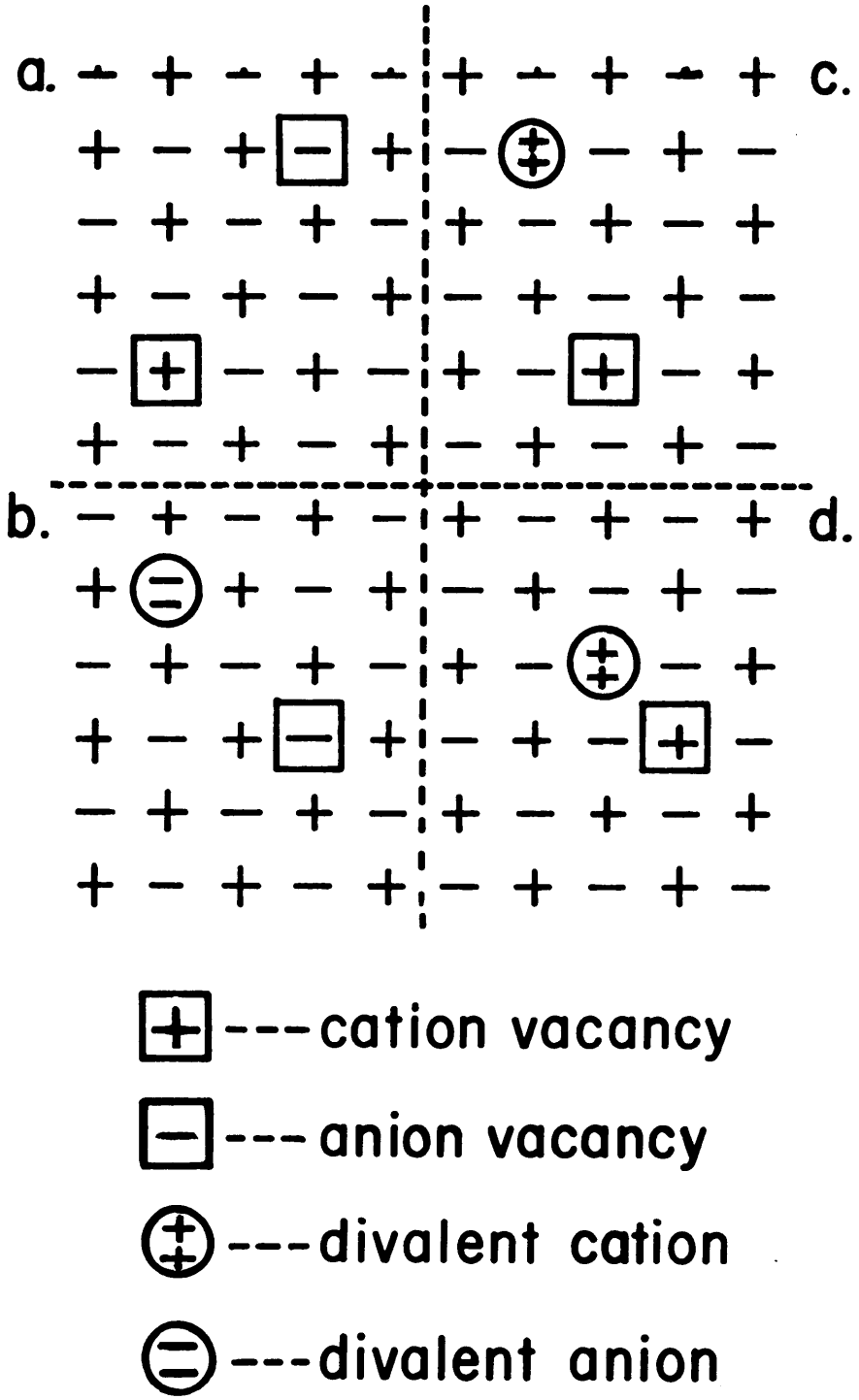

Figure 1.1. Two-dimensional representation of NaCl structure. a. Schottky pair. b. Divalent cation impurity. c. Divalent anion impurity. d. Impurity-vacancy complex.

that perfect order in a solid is not probable except at absolute zero. Point defects are introduced to disrupt the order. In the temperature range of these experiments, the point defect commonly found in the alkali halides is the Schottky pair. A Schottky pair is the absence of an anion and cation at their normal lattice sites. This absence is normally referred to as an anion or cation vacancy. The Schottky pair is illustrated in Figure (1.1a).

Absolute purity of most solids is technically impossible, so the position that an impurity ion occupies in the lattice must be considered. The impurities have been found to be substituted for the host cation or anion at their lattice sites. If an aliovalent impurity, which is an impurity with a valency differing from that of the corresponding ion of the host material, is introduced, a vacancy must also be formed to maintain charge neutrality as indicated in Figure (1.1b and c).

The vacancies may also provide for a mechanism of mass transport. This vacancy mechanism is simply the jumping of a cation to an adjacent, vacant cation site or an anion jumping to an adjacent, vacant anion site. The large amount of energy necessary to place a cation on an anion site, or vice versa, makes the probability of the cation and anion exchanging lattice sites very low. Since this problem is concerned with divalent cation diffusion in alkali halides, all reference to migration will be to this system of diffusion, unless otherwise indicated.

There have been no reported experiments contradicting the vacancy mechanism of mass transport in alkali halides with the NaCl structure. It is evident in this mechanism that the migration of a particular ion is dependent upon this ion having an adjacent vacancy. Thus, if the vacancy should be attracted to the site adjacent to this particular ion, the ion has a higher probability of motion than if it were to depend only on chance encounters with the vacancy.

Stasiw and Teltow (36) have postulated a model that leads to an attraction between a divalent cation and the cation vacancy. The basis of this model is the consideration of the ionic charge of the divalent cation and vacancy relative to the charge of the host cation in the alkali halide crystal. Hence, the divalent cation will appear to have a relative positive charge with respect to the lattice. The vacancy will appear to possess a relative negative charge since there is no charge where a positive charge normally existed. Because of the coulombic potential energy between the divalent impurity and the cation vacancy, the impurity-vacancy complex, illustrated in Figure (1.1b), should be formed. The existance of the impurity-vacancy complex has been verified through ESR studies carried out by Watkins (38).

Lidiard (25) has developed this association theory for the case of the diffusion of aliovalent impurities in ionic solids. His development indicates that under certain conditions the diffusion coefficient

should be a function of the diffusant concentration, if the association is valid. Results of diffusion experiments that confirm Lidiard's extension of the association theory have been reported by Keneshea and Fredericks (20, 22, 23). These experiments have the measurement of the Gibbs free energy of association of the impurity-vacancy complex as a primary purpose. As a result of determining the free energy, the saturation diffusion coefficient and the migration energy can be calculated.

While these early diffusion experiments did confirm the association theory, certain unexpected results and difficulties were noted by the experimenters and theoreticians. An anomalous surface effect was noted in many of these experiments (20, 22). Reisfeld, Glasner, and Honigbaum (31) questioned the work by Keneshea et al. (23) because the calculated Gibbs free energy of association was a rapidly varying function of the temperature. The effect of unintentional aliovalent impurities on the value of the free energy was discussed by the two groups (24, 31), but no conclusions could be drawn because of the lack of proper experimental studies of the subject. Howard and Lidiard (18) have developed an expression that treats a similar problem theoretically. However, their development only applies to the situation where the unintentional aliovalent impurity is the same ion as the diffusant and is present at a constant concentration in the crystal. Reisfeld et al. apply this expression to

experimental data (23) which the equation does not describe.

An investigation of the simultaneous diffusion of two divalent cations was chosen as a method to study the effect of unintentional aliovalent impurities on the diffusion of a divalent cation. Since the experimental data must be analyzed through the solution of a differential equation, it is important that the initial and boundary conditions be known for both the diffusant and the impurity. These necessary conditions can be controlled in the case of the simultaneous diffusion of two divalent cations.

Pb^{++} and Cd^{++} were chosen as the diffusants for several reasons. The first of which is that single ion diffusion studies had been carried out in this laboratory with these two cations (2, 3, 20, 22, 23, 28). Secondly, they possess sufficiently different ionic radii so they would not be expected to behave similarly in either NaCl or KCl. NaCl and KCl were used as the host materials since both were available in a purified form from this laboratory.

Although simultaneous diffusion seemed to be the method of experimentation without any obvious difficulties, the Stasiw-Teltow-Lidiard theory of association had to be adapted to a system which included two aliovalent impurities. Also, solutions of the diffusion equations for this new system had to be found. Solutions to Fick's second law of diffusion, when the concentration dependence of the diffusion coefficient is unknown, have been limited. The Matano

method (29) has been used to obtain the concentration dependent diffusion coefficients from the diffusion profiles of experiments conducted under specific initial and boundary conditions (2, 3, 20, 22, 23, 28). These diffusion coefficients are then used to calculate the Gibbs free energy of association. Such a two-step process may decrease the sensitivity and accuracy of the final result. Therefore, a solution, through which the parameters could be more directly related to the experimental data, was developed.

It was hoped that through this study a more accurate value of the Gibbs free energy of the impurity-vacancy association could be measured. If this is possible, the value of the migration energy would be improved.

II. THEORY

Since the formation of an impurity-vacancy complex affects the diffusion of aliovalent impurity ions in alkali halide crystals, it is necessary to determine what this effect may be. Lidiard (25) has done this for the case of a single species of impurity in an alkali halide crystal. The development for two ions will be similar to this single ion case.

Lidiard assumes, that if the complex has a sufficiently long life-time, the complex can be thought of as the diffusing particle. Fick's first law of diffusion can be written as

$$J = -D_s \, \partial(Npc)/\partial x. \qquad (2.1)$$

Where J is the flux of the complexes in the x direction with the units of complexes $cm^{-1}\ sec^{-1}$, D_s is the diffusion coefficient in terms of $cm^2\ sec^{-1}$, $\partial(Npc)/\partial x$ is the gradient of the complex concentration, N is the number of cations per cm^3, p is the degree of association, and c is the mole fraction of the aliovalent impurity. Equation (2.1) can be written in the following form.

$$J = -D_s \, [\partial(pc)/\partial c] \; \partial(Nc)/\partial x \qquad (2.2)$$

The impurity diffusion coefficient is

$$D(c) = D_s \, \partial(pc)/\partial c. \qquad (2.3)$$

D_s is frequently called the saturation diffusion coefficient of the impurity. It is the value of $D(c)$ when $p = 1$.

Equation (2.3) shows that the impurity diffusion coefficient is a function of the concentration. The next step is to determine the concentration dependence of p in the case of two aliovalent impurities.

The reactions necessary to form the two different complexes in the crystal are

$$Pb^{+} + V_c^{-} \rightleftharpoons PbV_c \qquad (2.4)$$

and

$$Cd^{+} + V_c^{-} \rightleftharpoons CdV_c. \qquad (2.5)$$

Where V_c^{-} represents a cation vacancy. It is emphasized that the charge is defined relative to the lattice. Through the use of statistical thermodynamics, mass action expressions similar to the following were derived by Lidiard (24).

$$[PbV_c]/[Pb^{+}][V_c^{-}] = 12 \exp(-\Delta G_{Pb}/kT) = K_{Pb} \qquad (2.6)$$

$$[CdV_c]/[Cd^{+}][V_c^{-}] = 12 \exp(-\Delta G_{Cd}/kT) = K_{Cd} \qquad (2.7)$$

The factor 12 is due to the number of distinct ways that the complex can be orientated in the NaCl lattice, and it is the configurational

entropy term. ΔG is the Gibbs free energy of the association reaction in the crystal, excluding the configuration entropy. All concentrations are in mole fractions.

These two equilibrium expressions contain the cation vacancy concentration in common. A vacancy cannot be directly observed, but the concentration of cation vacancies that results from the addition of the divalent cations is

$$[V_c^-] = [Pb\ ] + [Cd\ ] - [PbV_c] - [CdV_c] + [V_a^+]. \qquad (2.8)$$

Where $[V_a^+]$ is the concentration of anion vacancies in equilibrium with the cation vacancies. The expression governing this equilibrium is the Schottky product.

$$[V_c^-][V_a^+] = K_s = X_v^2 = B \exp(-W_s/kT) \qquad (2.9)$$

Where X_v is the mole fraction of cation or anion vacancies at equilibrium in a pure crystal, B is a ratio of entropy terms, and W_s is the energy required to form a Schottky pair.

If p_{Pb} and p_{Cd} are, respectively the fraction of Pb^{++} and Cd^{++} associated with a vacancy, the following expressions result from equations (2.6), (2.7) and (2.8).

$$[V_c^-] = p_{Pb}/K_{Pb}(1-p_{Pb}) \qquad (2.10)$$

$$[V_c^-] = p_{Cd}/K_{Cd}(1-p_{Cd}) \qquad (2.11)$$

$$[V_c^-] = (1-p_{Pb})[Pb] + (1-p_{Cd})[Cd] + [V_a^+] \qquad (2.12)$$

$[Pb]$ and $[Cd]$ represent the total concentration of lead and cadmium ions, respectively.

A cubic equation can be derived for both p_{Pb} and p_{Cd} from equations (2.10), (2.11) and (2.12). While an exact solution of a cubic equation is possible, a method of successive approximations is used to solve for p_{Pb} and p_{Cd}. The following operations are carried out until successive values of p_{Pb} and p_{Cd} agree in the sixth decimal place.

$$[ii] = (1-p_{Pb})[Pb] + (1-p_{Cd})[Cd] \qquad (2.13)$$

$$[V_a^+] = -[ii]/2 + ([ii]^2 + K_s)^{1/2}/2 \qquad (2.14)$$

$$p_{Pb} = K_{Pb}([ii] + [V_a^+])/1 + K_{Pb}([ii] + [V_a^+]) \qquad (2.15)$$

$$p_{Cd} = K_{Cd}([ii] + [V_a^+])/1 + K_{Cd}([ii] + [V_a^+]) \qquad (2.16)$$

An initial trial value of $p = 1/2$ is used.

In deriving these equations, certain assumptions must be made. For the mass action expressions to hold in the diffusion process, a localized equilibrium must exist everywhere in the crystal. Also, all interactions and aggregates except those mentioned are assumed to be negligible, and at the concentrations used and in the temperature ranges studied, this is true. The assumption, that the actual

diffusing species is the impurity-vacancy complex and not the impurity ion, has been introduced.

III. MATHEMATICAL SOLUTIONS

The experimental results are treated quantitatively through the solution of Fick's second law of diffusion. In the case of simultaneous diffusion, the following two coupled equations result when the complex is treated as the diffusing species.

$$\partial(p_{Pb}[Pb])/\partial t = \partial\{D_{s(Pb)}\partial(p_{Pb}[Pb])/\partial x\}/\partial x \qquad (3.1)$$

$$\partial(p_{Cd}[Cd])/\partial t = \partial\{D_{s(Cd)}\partial(p_{Cd}[Cd])/\partial x\}/\partial x \qquad (3.2)$$

The Schmidt method (33) of finite differences was chosen as the mode of solution. This method is performed in such a manner as to simultaneously solve the coupled differential equations. Finite differences has been well discussed in several texts (6, 7, 8, 10), but a brief introduction is given here.

Fick's second law written in general form is

$$\partial c/\partial t = \partial(D\partial c/\partial x)/\partial x. \qquad (3.3)$$

If D is a constant and the following dimensionless parameters are introduced,

$$X = x/b, \quad Z = Dt/b^2 \quad \text{and} \quad C = c/c_o, \qquad (3.4)$$

equation (3.3) can be written as

$$\partial C/\partial T = \partial^2 C/\partial X^2. \qquad (3.5)$$

Where b is a constant distance, and c_o is the concentration at the surface.

Let C_{m+1}, C_m, C_{m-1} be the average concentrations in the space intervals $(m+1)\delta X$, $m\delta X$, $(m-1)\delta X$, respectively, and C'_m, C_m be the average concentrations in the space interval $m\delta X$ at the time intervals $(m+1)\delta Z$, $m\delta Z$, respectively. Using these definitions and a Taylor series to expand C_{m+1}, C_{m-1} and C'_m, these concentrations can be expressed as

$$C_{m+1} = C_m + \delta X(\partial C/\partial X)_m + 1/2(\delta X)^2(\partial^2 C/\partial X^2)_m + \ldots, \qquad (3.6)$$

$$C_{m-1} = C_m - \delta X(\partial C/\partial X)_m + 1/2(\delta X)^2(\partial^2 C/\partial X^2)_m - \ldots \qquad (3.7)$$

and

$$C'_m = C_m - \delta Z(\partial C/\partial Z)_m + 1/2(\delta Z)^2(\partial^2 C/\partial Z^2)_m + \ldots . \qquad (3.8)$$

By adding equations (3.6) and (3.7), the following relationship results if the fourth and higher order terms are dropped.

$$(\partial^2 C/\partial X^2)_m = (C_{m+1} - 2C_m + C_{m-1})/(\delta X)^2 \qquad (3.9)$$

Similarly, by neglecting the second and higher order terms in equation (3.8), the following equation results.

$$(\partial C/\partial Z)_m = (C'_m - C_m)/\delta Z \qquad (3.10)$$

Equations (3.9) and (3.10) are combined as indicated by equation (3.5) to give

$$C'_m = C_m + \delta Z/(\delta X)^2 (C_{m+1} - 2C_m + C_{m-1}). \qquad (3.11)$$

Inserting the original parameters (3.4), equation (3.11) becomes

$$C'_m = c_m + D\delta t/(\delta x)^2 (c_{m+1} - 2c_m + c_{m-1}). \qquad (3.12)$$

Use of this formulation is the Schmidt method of finite differences. The validity of dropping the higher order terms is checked by comparing one generated profile with another which has been generated by using smaller intervals of time and space. Since the two profiles were found to agree in the fourth significant figure when using the parameters used in this study, the procedure of dropping higher order terms is valid. This solution is found to be stable as long as the ratio $D\delta t/(\delta x)^2$ is chosen to be one-half or less (10).

By introducing the impurity-vacancy complex as the diffusing species, equation (3.12) becomes

$$[Pb]'_m = [Pb]_m + D_{s(Pb)} \delta t/(\delta x)^2 \{(p_{Pb}[Pb])_{m+1} - 2(p_{Pb}[Pb])_m + (p_{Pb}[Pb])_{m-1}\} \qquad (3.13)$$

for the lead ions and

$$[Cd]'_m = [Cd]_m + D_{s(Cd)}\,\delta t/(\delta x)^2 \{(p_{Cd}[Cd])_{m+1} - 2(p_{Cd}[Cd])_m + (p_{Cd}[Cd])_{m-1}\} \tag{3.14}$$

for the cadmium ions. Seemingly, two different symbols have been introduced for c_m, but it is pointed out that $[Pb]'_m$ and $[Pb]_m$ are accumulative terms, and the remaining terms govern the diffusion process.

When the time and space intervals are selected to be identical in both equations, the diffusion profiles generated by the use of equations (3.13) and (3.14) are the simultaneous solutions of the differential equations (3.1) and (3.2). The initial and boundary conditions are

$$\begin{aligned} &c = 0 \quad \text{for} \quad x \geq 0 \quad \text{at} \quad t = 0, \\ &C = C_1 \quad \text{for} \quad t > 0 \quad \text{at} \quad x = 0, \\ &\partial C/\partial x = 0 \quad \text{at} \quad x = \infty \quad \text{and} \quad t = t_t. \end{aligned} \tag{3.15}$$

Where t_t is the total time of the diffusion anneal, and C_1 is a constant concentration. Figure (3.1) is a block diagram of the computer program used to generate the diffusion profiles.

Since no analytic solution of the coupled differential equations exists, there is no check of the correctness of the generated profiles except by comparison to other profiles generated by using

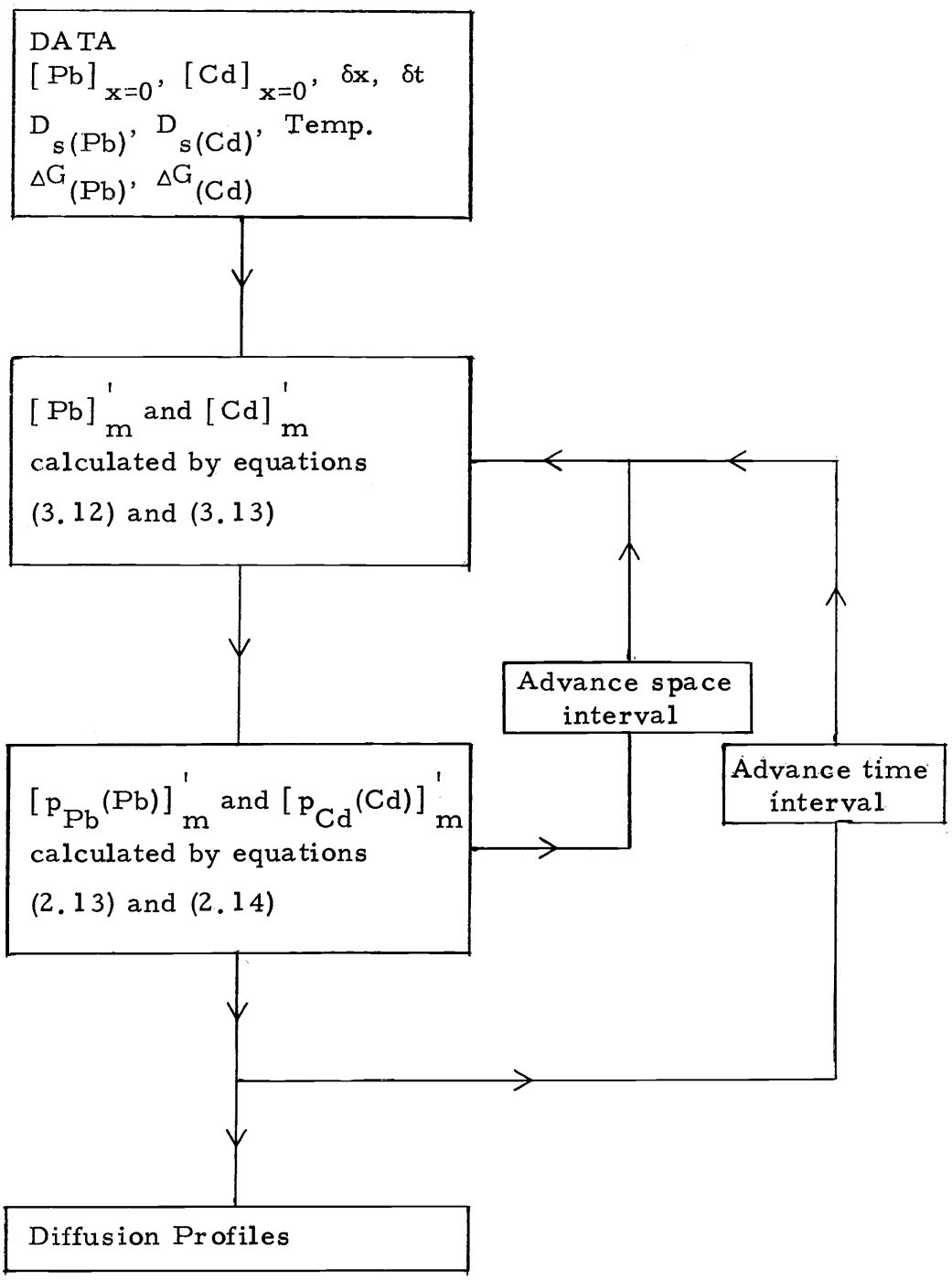

Figure 3.1 Block diagram of the computer program used to generate the simultaneous profiles.

smaller intervals of time and space. However, the validity of this formulation in treating the concentration dependent diffusion coefficient can be shown in the case of a single aliovalent impurity diffusion.

Figure (3.2) shows three profiles generated by equations (3.13) and (3.14) when $[Pb]_{x=0} = 0$. Matano's method (29) is used to calculate the concentration dependent diffusion coefficient through the use of the following equation (21, p. 17-18).

$$D(c) = - \int_{o}^{c} x dc' / 2t_t \left| \partial C' / \partial x \right|_c \qquad (3.16)$$

The integration and differentiation of the generated profiles must be done graphically. An expression relating $D(c)$ to the association theory has been derived by Lidiard (25), and it is

$$D(c) = D_s \{1 - (1 + 48c \exp(\Delta G/kT))^{-1/2}\} . \qquad (3.17)$$

These two independent solutions to $D(c)$, (3.16) and (3.17), are compared by plotting $D(c)/D_s$ versus c in Figure (3.3). These solutions agree within the scatter introduced by the graphical operations involved in the solution of equation (3.16).

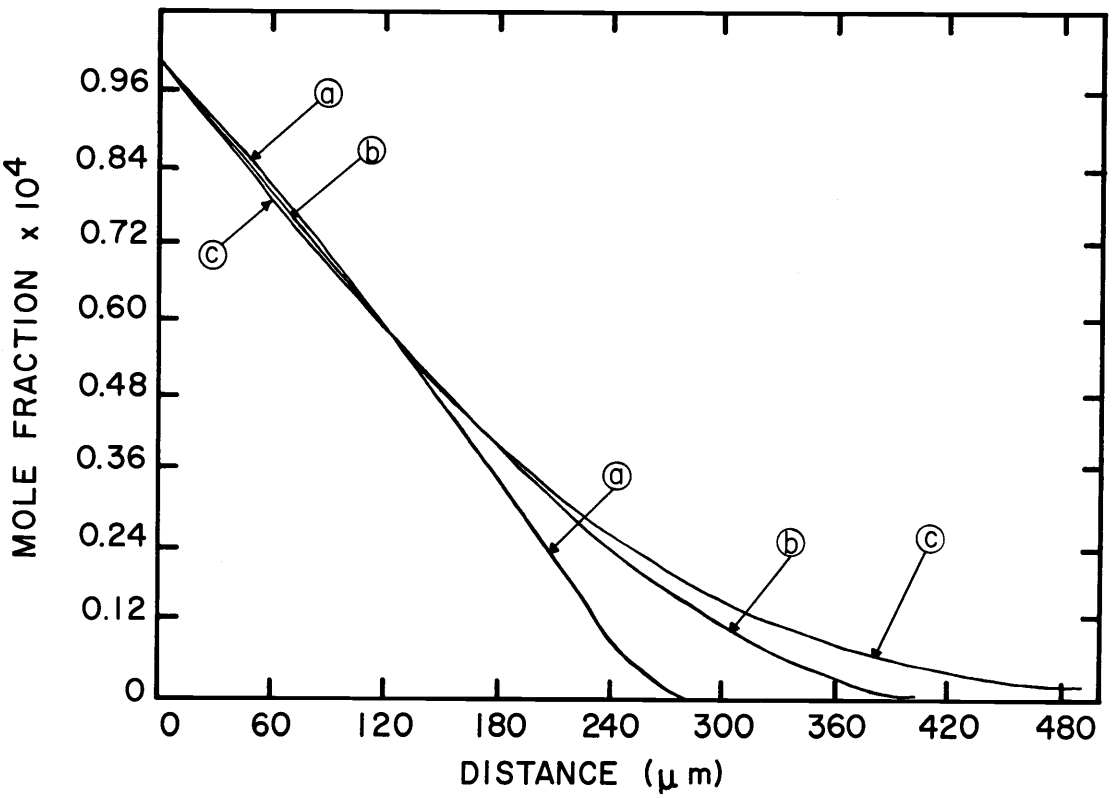

Figure 3.2. Diffusion profiles of divalent cations generated by the Schmidt method of finite differences. $t_t = 5 \times 10^5$ sec. Temperature = 452°C.

a. $D_s = 2.02 \times 10^{-09}$ cm^2/sec $\Delta G = -0.30$ev

b. $D_s = 6.00 \times 10^{-10}$ cm^2/sec $\Delta G = -0.50$ev

c. $D_s = 4.85 \times 10^{-10}$ cm^2/sec $\Delta G = -0.70$ev

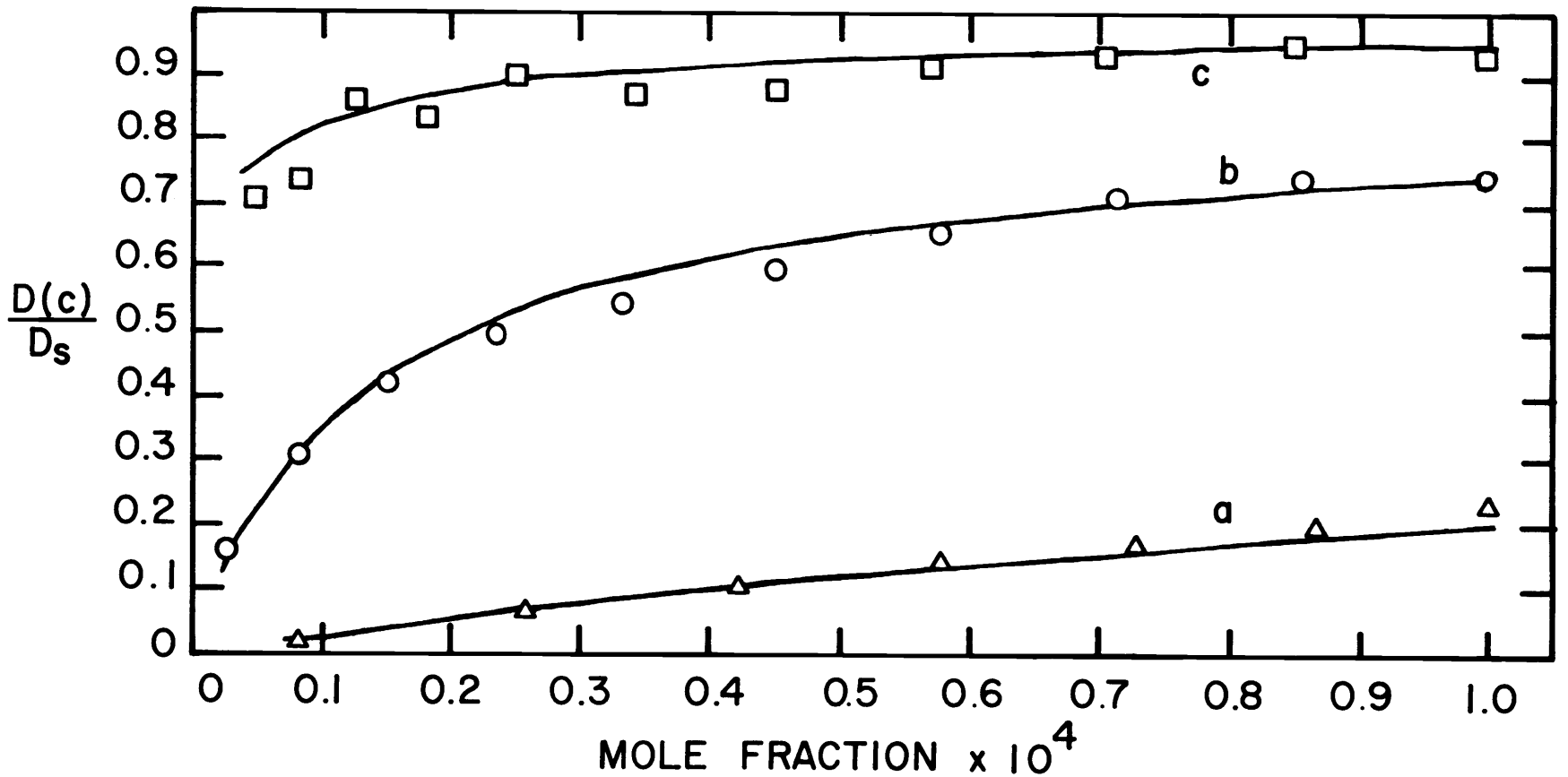

Figure 3.3. Comparison of $D(c)/D_s$ calculated from the profiles of Figure (3.2) by the Matano method and the theoretical $D(c)/D_s$ (solid line) calculated from the association theory. $t_t = t \times 10^5$sec. Temperature = 452°C.

a. $D_s = 2.02 \times 10^{-09}$ cm^2/sec $\Delta G = -0.30$ev b. $D_s = 6.00 \times 10^{-10}$ cm^2/sec $\Delta G = -0.50$ev

c. $D_s = 4.85 \times 10^{-10}$ cm^2/sec $\Delta G = -0.70$ev

IV. EXPERIMENTAL

Single crystals of NaCl and KCl were grown from reagent grade salts that had been purified by an ion-exchange method (10, p. 3, 4; 11, p. 3-14). Results of preliminary analysis (34) of crystals grown from this purified salt are shown in Table (4.1).

The purified KCl was heated to 200°C and dried by alternately adding HCl and evacuating the system. After the salt was dry, it was melted under an atmosphere of Cl_2. Then HCl (1/6 atm) was reintroduced and the Vycor growth tube was sealed. A single crystal was grown by the Stockbarger-Bridgman method.

Since the NaCl single crystals grown by the Stockbarger-Bridgman method were badly strained, these crystals were grown by the Kyropoulas method. The salt was dried in the same manner as KCl, but it was melted under an atmosphere of HCl. An atmosphere (>1 atm) of Ar and HCl was used while growing the crystal. Both NaCl and KCl single crystals were annealed from 650°C at a rate of less than a degree per minute in an atmosphere of Cl_2 (1/3 atm).

The maximum concentration of OH^- in the NaCl was calculated to be 0.23 ppm by using the height of the absorbtion peak at 185 nm (16). No other absorbtion peaks in the range 800 to 185 nm were observed in the NaCl crystals. An upper limit of 0.01 ppm was

Table 4.1. Characteristics of KCl crystals and KCl crystals grown by the Kyropoulus method from O.S.U. purified salts from data collected by L. Schuerman (34).

Impurity Ion	O.S.U. KCl	Reagent KCl	Harshaw KCl	O.S.U. NaCl	Method[b]
			(ppm)		
Ag^{+}	0.001[a]	N.A.	N.A.	0.01[a]	1
Br^{-}	3-4	35	10	0.95	2
BO_2^{-}	0.01[a]	8	1	N.A.	1
Cd^{+2}	1.0[a]	1.3	N.A.	N.A.	3
I^{-}	0.4[a]	~0.4	N.A.	N.A.	1
K^{+}	N.A.	N.A.	N.A.	1[a]	2
Mg^{+2}	0.5[a]	0.8	N.A.	N.A.	3
Mn^{+2}	0.004[a]	0.004[a]	0.009	.004[a]	2
Na^{+}	3-4	40-50	2.5-4.0	N.A.	2
OH^{-}	0.001[a]	N.A.	1.5-10	0.23	1
Pb^{+2}	0.004[a]	0.5	0.05	0.01[a]	1
Rb^{+}	6.0	N.A.	2.8-5.0	N.A.	2
Tl^{+}	0.001[a]	N.A.	N.A.	0.01[a]	1

[a] Set by the detection limit of analytical method.

N.A. = Not analyzed.

[b] 1. Optical absorption 2. Activation analysis 3. Atomic absorption.

placed on the OH^- concentration in the KCl crystals since no absorbtion peaks were detected in the above stated region.

Carrier free Pb-210 and Cd-109 were obtained from the New England Nuclear Corporation. The specific activity for the $Pb(NO_3)_2$ was 5.0 mC/mg and for the $CdCl_2$ was 3.8 mC/mg. A 99+% radiometric purity was listed for both isotopes.

The diffusion ampoule and crystal are shown in Figure (4.1). $PbCl_2$ and $CdCl_2$ carrier and tracer solutions were evaporated to dryness in the ampoule. This was done by flowing N_2 over the surface of the hydrochloric solutions while heating the solutions at 70°C. The ratio of tracer to carrier was 0.080 mC/mg for the $PbCl_2$ and 0.129 mC/mg for the $CdCl_2$. One-sixth to one-third atmosphere of Cl_2 was sealed in the ampoule to force the following equilibrium to the left through the application of LeChatelier's principle.

$$2\ CdCl_2 \rightleftharpoons 2\ CdCl + Cl_2 \qquad (4.1)$$

Figure (4.2) shows the diffusion anneal apparatus. The temperature of the sample was constant within ±1°C, and the bottom of the diffusion ampoule was 5°C cooler than the crystal or the top of the tube after one hour or less. A check of the temperature of the carbon block and the inside of an open tube showed that it differed by less than 1°C. These temperatures were measured with a Pt-Pt 13% Rh thermocouple which had been calibrated by Charles Allen

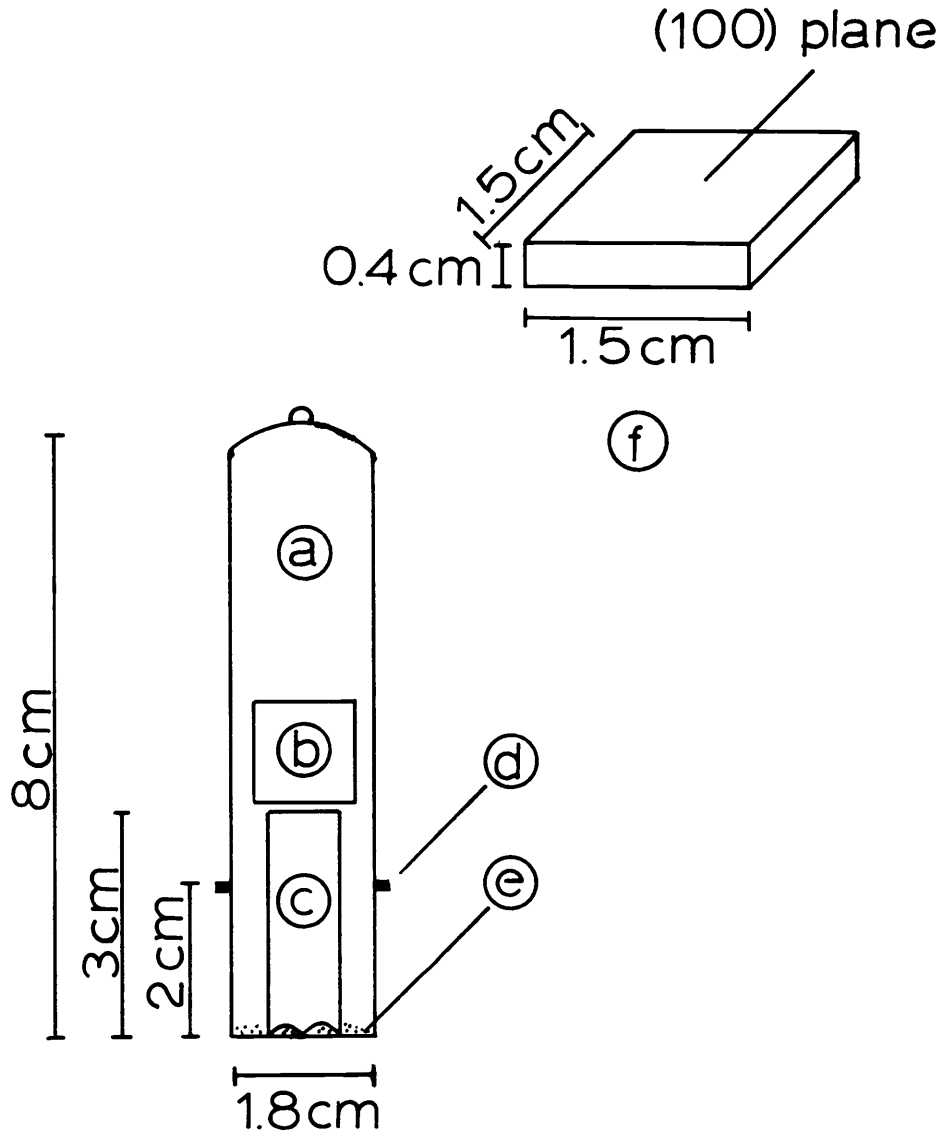

Figure 4.1. Diffusion ampoule and crystal. Dimensions are average values of those used in the experiments. a. Vycor tube. b. Crystal. c. Pedestal. d. Positioning projections. e. Diffusant. f. Enlarged diagram of crystal.

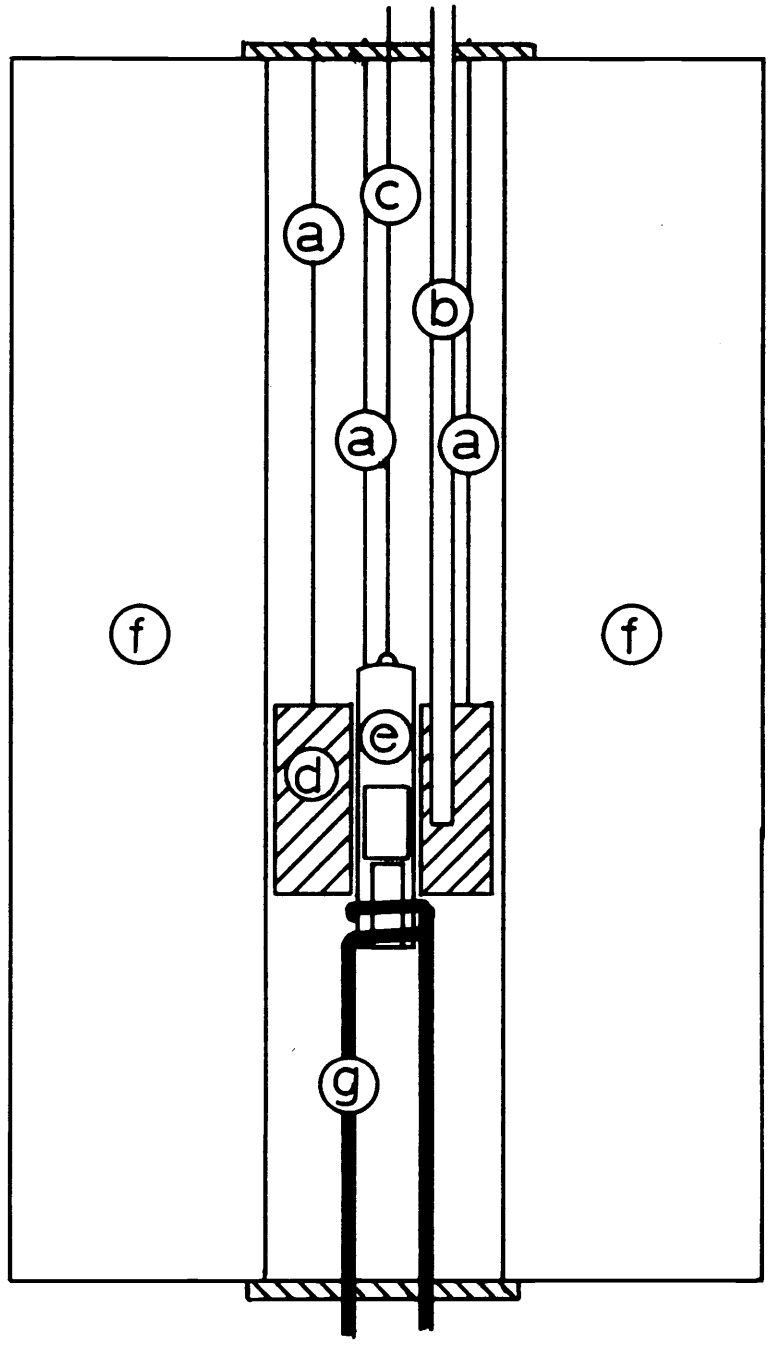

Figure 4.2. Diffusion anneal apparatus. a. Support wires for carbon block. b. Thermocouple. c. Support wire for ampoule. d. Carbon block. e. Ampoule. f. Furnace. g. Cooling coil.

(1, p. 19).

The source of the diffusant at the surface of the crystal is the vapor. As long as the condensed phase remains in the ampoule, the vapor pressure will remain constant. Ten times the necessary amount of the diffusant was used to insure that the diffusant would be in excess. Therefore, the boundary conditions introduced in (3.15) are met.

After the diffusion anneal, the crystal or crystals were removed from the ampoule. Two millimeter sections were cleaved from the four edges of the crystal to insure that the diffusion process would be one dimensional. Two samples were obtained from most anneals for comparison. Either two crystals were initially introduced in the diffusion ampoule, or more often, the one crystal was divided in half by cleaving the crystal parallel to the (100) plane after the diffusion anneal, Figure (4.2).

The crystals were sectioned by using an American Optical Company Model 960 Microtome. These sections were collected in preweighed vials which had been cleaned with a chromic acid solution and rinsed several times with deionized water to remove the chromic acid. Both samples and vials were dried at 110°C for three hours before being weighed on a Mettler microbalance.

The gamma radiation of Pb-210 and Cd-109 was counted with a Packard Model 410A Auto-Gamma Spectrometer. The 86 Kev

photopeak of Cd-109 and the 46 Kev photopeak of Pb-210 were counted while using a 20 Kev window. Unfortunately, there was a slight overlap of the two peaks, and the following equations were used to find the corrected activity.

$$A_{Pb} = A_{46Kev} - A_{86Kev}A_{46Kev}(\text{Cd St.})/A_{86Kev}(\text{Cd St.}) \quad (4.2)$$

$$A_{Cd} = A_{86Kev} - A_{46Kev}A_{86Kev}(\text{Pb St.})/A_{46Kev}(\text{Pb St.}) \quad (4.3)$$

Where A represents the activity and the subscript indicates which channel was counted.

These corrections were used for the NaCl experiments, but they could not be used for the KCl experiments. This is because the surface concentration of Cd^{++} is one-tenth or less that of Pb^{++} in the KCl. Therefore, a small error in the ratio $\{A_{86Kev}(\text{Pb St.})/A_{46Kev}(\text{Pb St.})\}$ or in A_{46Kev} will cause a large error in A_{Cd}.

A chemical separation of Cd^{++} and Pb^{++} was used to find the concentration of Cd^{++} in some KCl experiments. Both $Cd(OH)_2$ and $Pb(OH)_2$ are insoluble, but Cd^{++} forms a complex $\{Cd(NH_3)_4^{++}\}$ in an ammonia solution. $Pb(NO_3)_2$ and $Cd(NO_3)_2$ carriers were added to each sample to insure completeness of separation. A 28% ammonia solution was used to wash the precipitate. This solution, which contained the cadmium complex, was evaporated

to dryness by placing the test tubes in a heated carbon block and blowing air across the mouths of the tubes.

After the activity of each ion had been determined, the mole fractions of the ions were calculated by the following equation.

$$\text{Mole fraction}_M = A_M MW_{solvent} C_c V_c V_{St.} / (MW_{solute} V_t A_{St.} w) \quad (4.4)$$

Where C_c and V_c are the concentration and volume of the carrier used in the experiment, V_t is the volume of the tracer solution used, $V_{St.}$ is the volume of the tracer solution used in making the standard, and w is the weight of the sample.

Several experimental problems were encountered during the diffusion anneal. One of these problems was that the two samples of each anneal had differing surface concentration of Cd^{++} as illustrated in Figure (4.3). This would not be expected if the source of the diffusant was the vapor. There seemed to be several possible causes of this problem. One is that the temperature is not uniform in the diffusion ampoule. The carbon block illustrated in Figure (4.2) was to insure a uniform temperature.

Since the crystal would be much colder than the diffusant during the initial warmup period, another possibility is that the diffusant was transferred from the bottom of the tube and deposited on the crystal surface. As an attempted solution, the water cooled coil shown in Figure (4.2) was used to keep the diffusant at a low

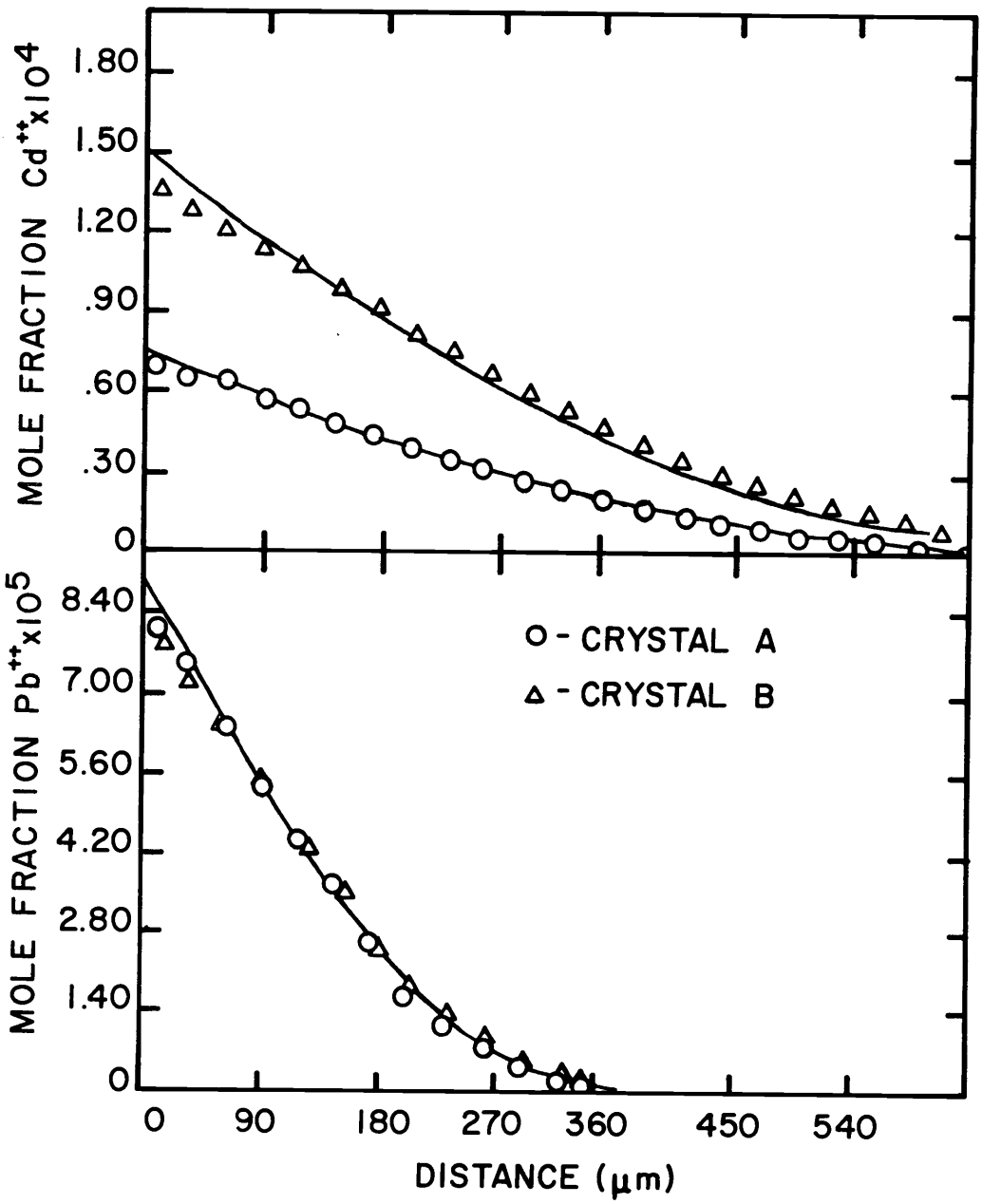

Figure 4.3. Penetration profiles in NaCl showing the differing surface concentrations of Cd^{++}. $t_t = 1.1239 \times 10^5$ sec. Temperature = 347°C.

(100° to 150°C) temperature while the crystal was brought to the anneal temperature. After 15 to 20 minutes the cooling coil was removed, and this time was recorded as time zero. The comparison profiles agreed within experimental error in all later experiments except two at 360°C and 409°C in NaCl. A reason for the exceptions is not known.

A problem observed in the KCl experiments was the formation of a second phase on the surface of the crystal during the diffusion anneal. Brand (5) in a phase study of the KCl-$CdCl_2$ system reported the congruent melting compound $KCdCl_3$. The solution was to mix KCl with the diffusant on the bottom of the ampoule, and then the compound is formed on the bottom of the ampoule and not on the crystal surface. Due to the change of the chemical potential of the Cd^{++}, the surface concentration of Cd^{++} is much lower than in NaCl; however, the boundary conditions are met.

It was observed that the concentrations of the diffusants in the first few slices were lower than expected. Such an effect could be accounted for by desorption after the diffusion ampoule was removed from the furnace. The diffusant on the bottom of the ampoule would cool rapidly because of contact with the walls of the ampoule, but the crystal, having little contact with the walls, would cool more slowly. The diffusion ampoule was dropped into ice water and then placed in liquid nitrogen in an effort to quench the crystal more rapidly.

While this method of quenching did offer some improvement over quenching in air, it did not completely stop the desorption as is discussed in the next section.

V. RESULTS

Potassium Chloride

Values of the saturation diffusion coefficients and the Gibbs free energies of association for the Pb^{++}- and Cd^{++}-vacancy complexes were chosen so that the profiles generated by the Schmidt method fit within experimental error a major section of the experimental profiles. Figures (5.1) through (5.6) show these profiles for the KCl experiments. The values of the parameters used to calculate the profiles are listed in Table (5.1). In KCl the thermal vacancies were considered in the calculations, and K_s (equation 2.09) was expressed as

$$K_s = 43.91 \exp(-2.313 \text{ ev}/2kT), \tag{5.1}$$

which is from the thesis of Fuller (14, p. 32).

In the fitting of the profiles, it was found that the section of the Cd^{++} profile beyond the point where $[Cd] = [Pb]$ was the most critical in determining the parameters. The sections of the profile noted in Figure (5.7) are shown as evidence of this, and also, note that the shapes of the Pb^{++} profiles in Figure (5.8) are important in determining the value of ΔG_{Pb}. Since the Pb^{++} only penetrates one-fourth as far into the crystal as the Cd^{++}, a major section of the

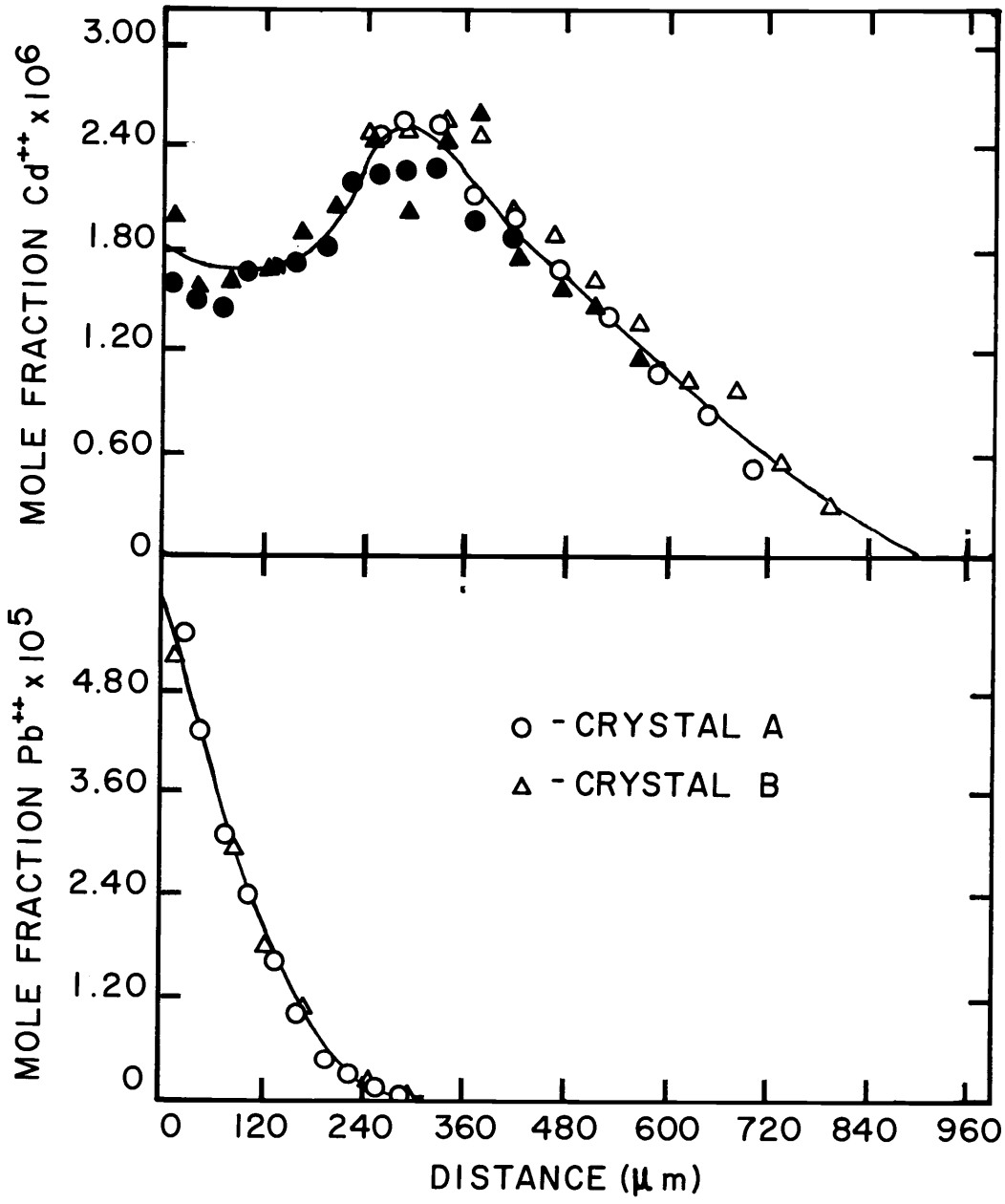

Figure 5.1. Penetration profiles for the diffusion of cadmium and lead ions in KCl at 367°C. $t_t = 1.6640 \times 10^6$ sec. Filled in symbols represent separated Cd^{++}. Solid curves are profiles generated by finite differences using the following parameters.

$D_{s(Cd)} = 1.70 \times 10^{-09}$ cm^2/sec $\quad \Delta G_{Cd} = -0.555$ev

$D_{s(Pb)} = 7.00 \times 10^{-11}$ cm^2/sec $\quad \Delta G_{Pb} = -0.480$ev

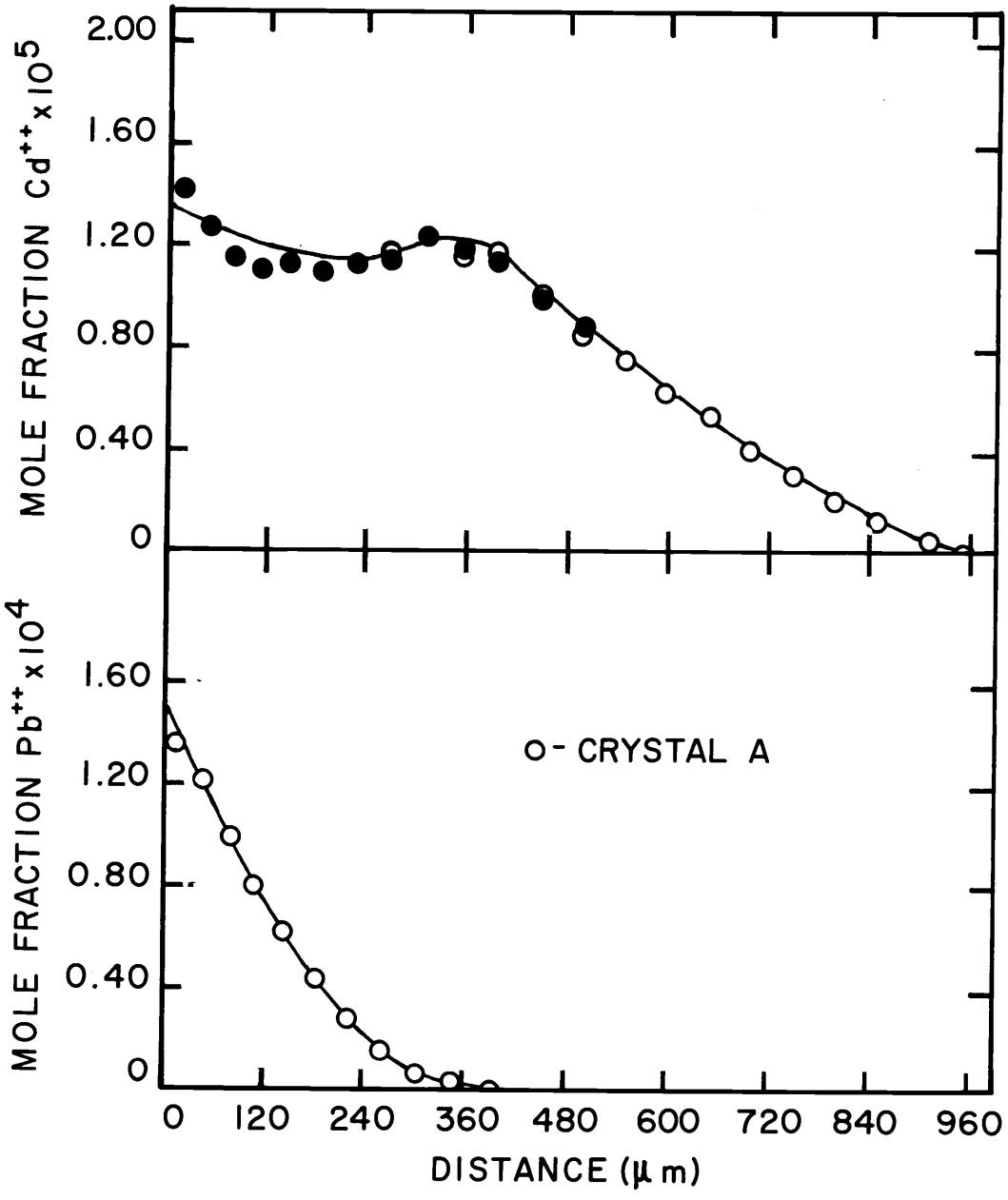

Figure 5.2. Penetration profiles for the diffusion of cadmium and lead ions in KCl at 455°C. $t_t = 3.9200 \times 10^5$ sec. Filled in symbols represent separated Cd^{++}. Solid curves are profiles generated by finite differences using the following parameters.

$D_{s(Cd)} = 5.80 \times 10^{-09} cm^2/sec \quad \Delta G_{Cd} = -0.562 ev$

$D_{s(Pb)} = 5.15 \times 10^{-10} cm^2/sec \quad \Delta G_{Pb} = -0.495 ev$

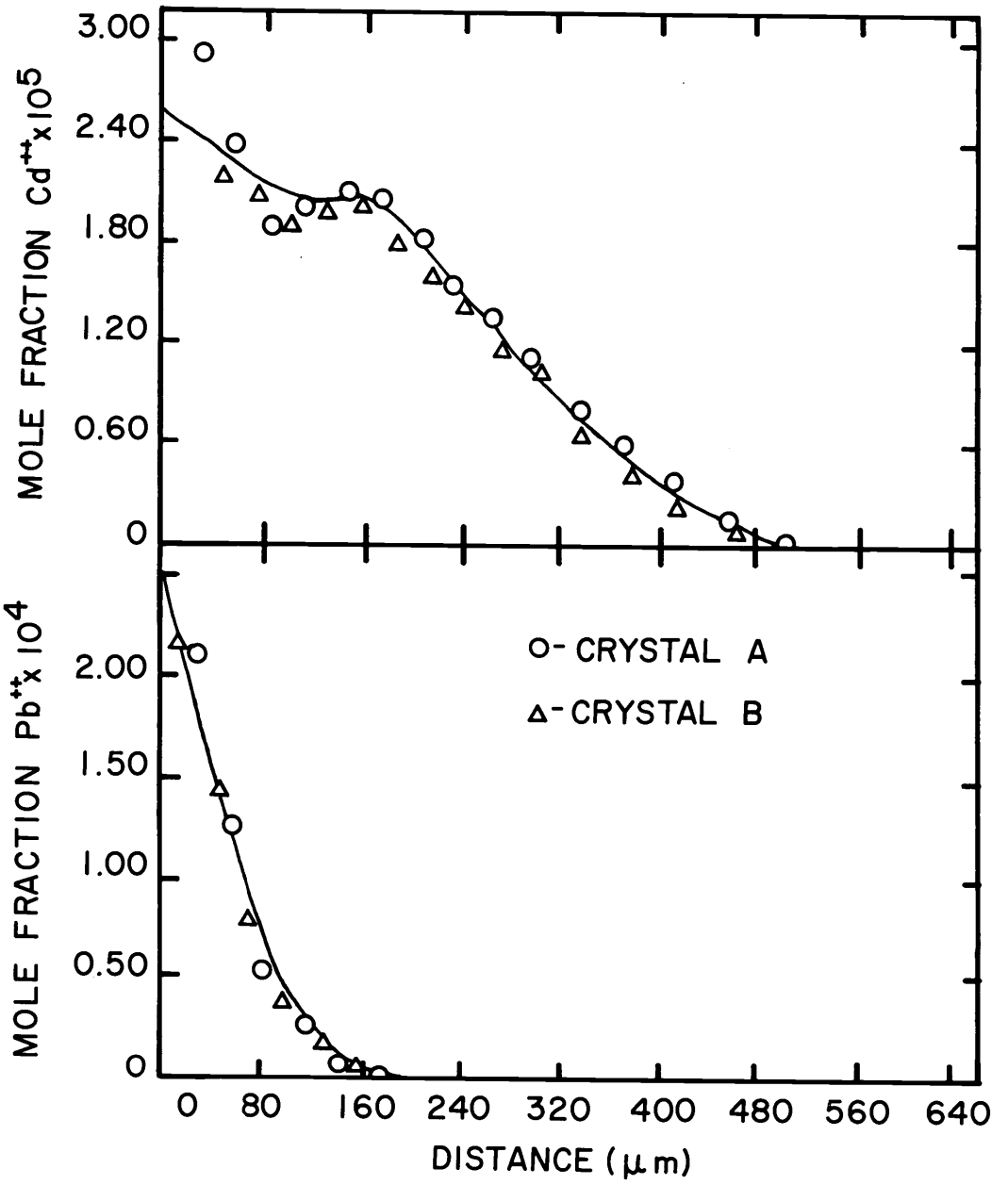

Figure 5.3. Penetration profiles for the diffusion of cadmium and lead ions in KCl at 458°C. $t_t = 8.336 \times 10^4$ sec. Solid curves are profiles generated by finite differences using the following parameters.

$D_{s(Cd)} = 5.70 \times 10^{-09}$ cm^2/sec $\quad \Delta G_{Cd} = -0.563$ev

$D_{s(Pb)} = 5.40 \times 10^{-10}$ cm^2/sec $\quad \Delta G_{Pb} = -0.495$ev

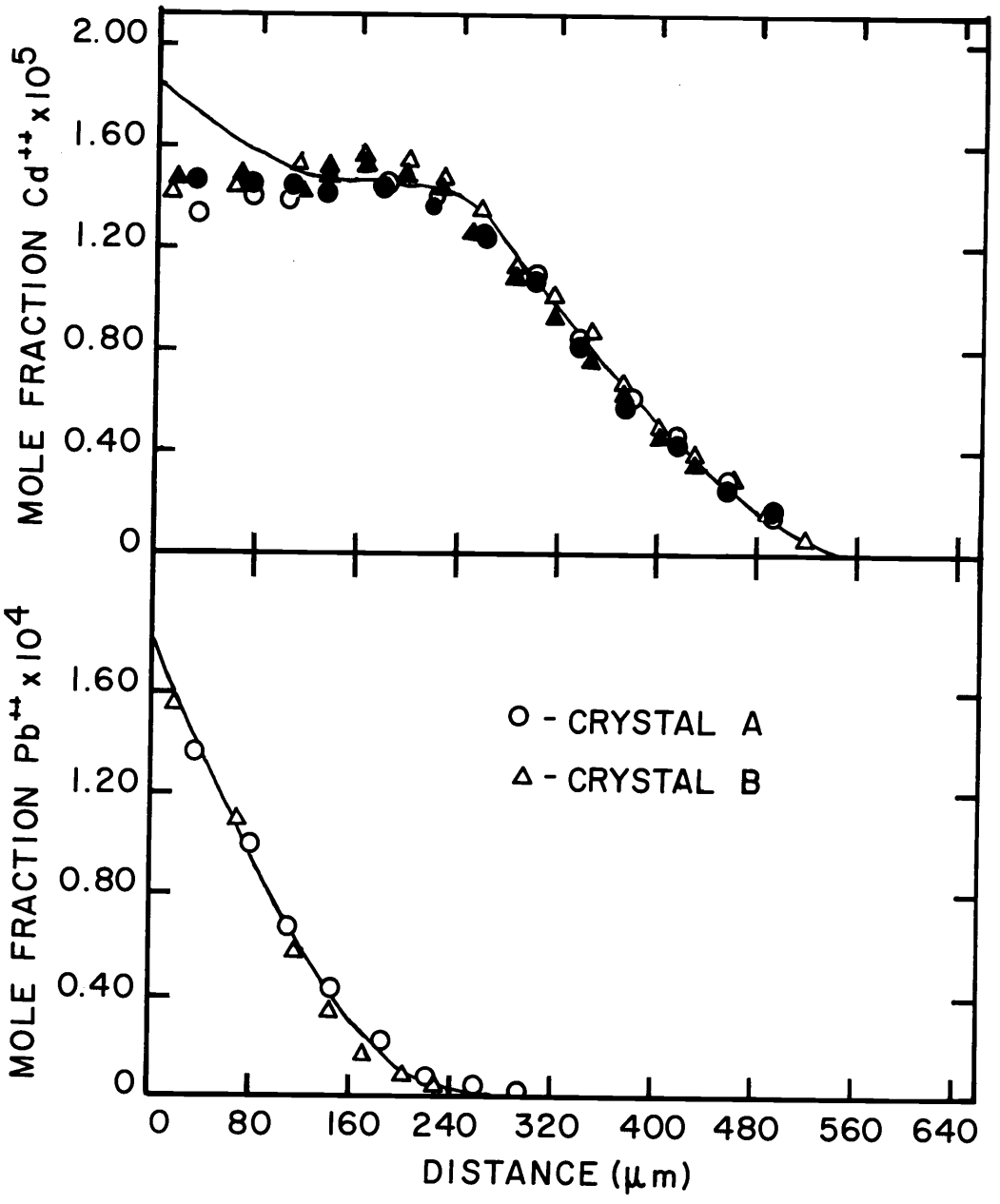

Figure 5.4. Penetration profiles for the diffusion of cadmium and lead ions in KCl at 492°C. $t_t = 8.6800 \times 10^5$sec. Filled in symbols represent separated Cd^{++}. Solid curves are profiles generated by finite differences using the following parameters.

$D_{s(Cd)} = 8.10 \times 10^{-09} cm^2/sec \quad \Delta G_{Cd} = -0.565ev$

$D_{s(Pb)} = 1.15 \times 10^{-09} cm^2/sec \quad \Delta G_{Pb} = -0.500ev$

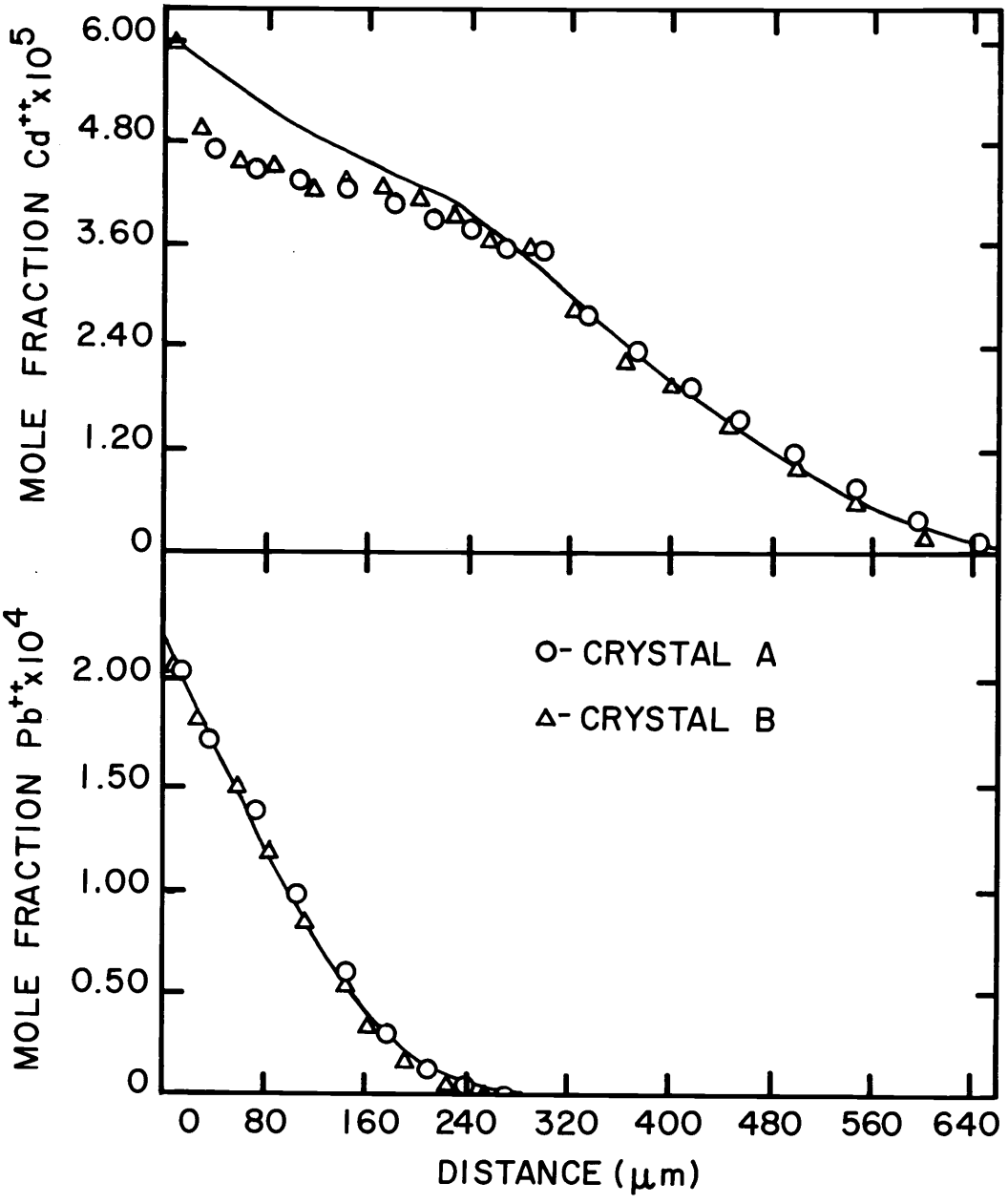

Figure 5.5. Penetration profiles for the diffusion of cadmium and lead ions in KCl at 509°C. $t_t = 7.292 \times 10^4$sec. Solid curves are profiles generated by finite differences using the following parameters.

$D_{s(Cd)} = 1.05 \times 10^{-08}$ cm^2/sec $\quad \Delta G_{Cd} = -0.572$ev

$D_{s(Pb)} = 1.45 \times 10^{-09}$ cm^2/sec $\quad \Delta G_{Pb} = -0.503$ev

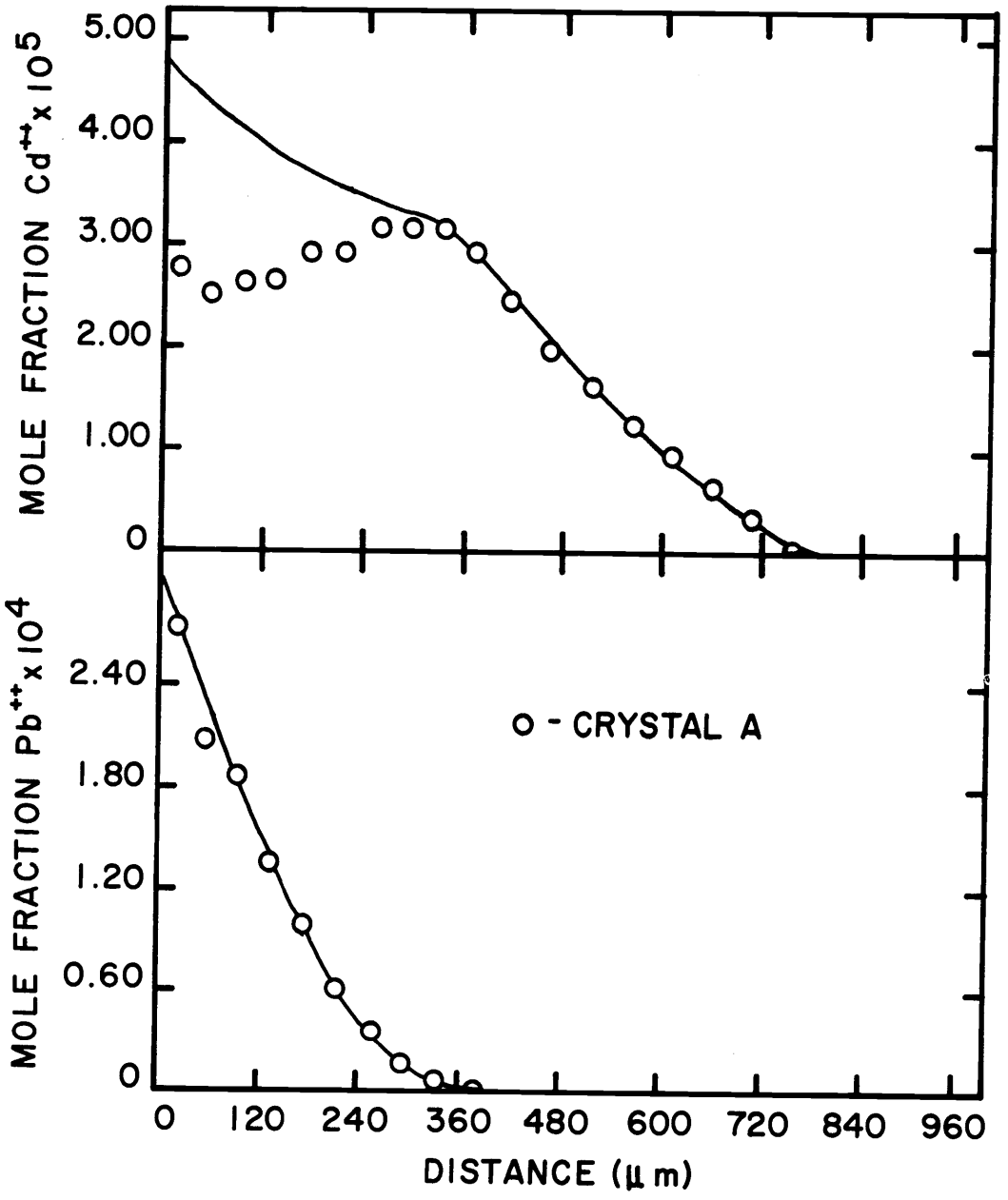

Figure 5.6. Penetration profiles for the diffusion of cadmium and lead ions in KCl at 553°C. $t_t = 7.716 \times 10^4$sec. Solid curves are profiles generated by finite differences using the following parameters.

$D_{s(Cd)} = 1.70 \times 10^{-08} cm^2/sec \quad \Delta G_{Cd} = -0.578ev$

$D_{s(Pb)} = 2.70 \times 10^{-09} cm^2/sec \quad \Delta G_{Pb} = -0.510ev$

Table 5.1. Values of D_s and ΔG used to generate diffusion profiles of Pb^{++} and Cd^{++} in KCl.

T (°C)	$D_{s(Pb)}$ (cm^2/sec)	$D_{s(Cd)}$ (cm^2/sec)	ΔG_{Pb} (ev)	ΔG_{Cd} (ev)	Notes
367	7.00×10^{-11}	1.70×10^{-09}	-0.480	-0.555	a, b, c
455	5.15×10^{-10}	5.80×10^{-09}	-0.495	-0.562	a, c
458	5.40×10^{-10}	5.70×10^{-09}	-0.495	-0.563	a, b, d
492	1.15×10^{-09}	8.10×10^{-09}	-0.500	-0.565	a, b, c
509	1.45×10^{-09}	1.05×10^{-08}	-0.503	-0.572	a, b, d
553	2.70×10^{-09}	1.70×10^{-08}	-0.510	-0.578	a
450	5.40×10^{-10}	5.70×10^{-09}	-0.495	-0.563	b, e

a. Crystal A
b. Crystal B
c. Cadmium chemically separated.
d. Second phase on surface of crystal.
e. Desorption study on crystal from 458°C.

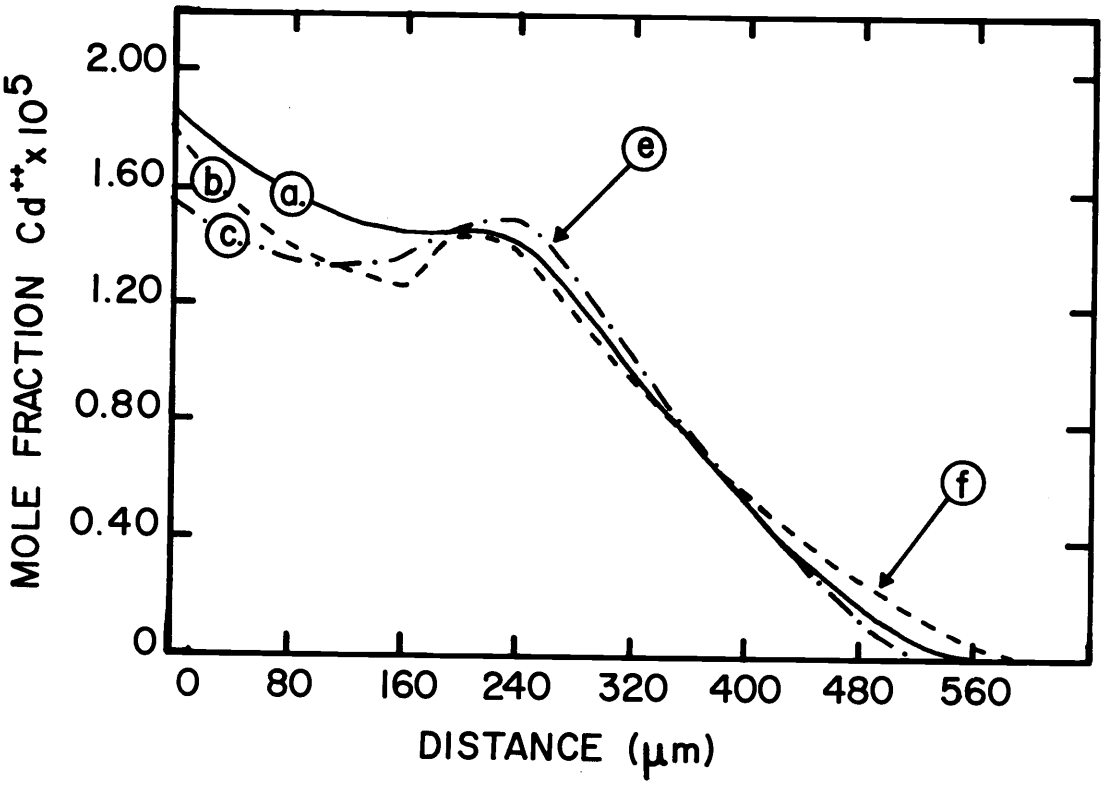

Figure 5.7. Trial profiles used in determining correct parameters to fit Cd^{++} profiles in KCl. Sections e. and f. of the profiles are important. Curve a. is profile used to fit the experimental data in Figure (5.4). $T = 492^{\circ}C$, $t_t = 8.6800 \times 10^5$ sec.

a. $D_{s(Cd)} = 8.10 \times 10^{-09}\ cm^2/sec$ $\Delta G_{Cd} = -0.565ev$
$D_{s(Pb)} = 1.15 \times 10^{-09}\ cm^2/sec$ $\Delta G_{Pb} = -0.500ev$

b. $D_{s(Cd)} = 8.00 \times 10^{-09}\ cm^2/sec$ $\Delta G_{Cd} = -0.600ev$
$D_{s(Pb)} = 1.90 \times 10^{-09}\ cm^2/sec$ $\Delta G_{Pb} = -0.400ev$

c. $D_{s(Cd)} = 1.00 \times 10^{-08}\ cm^2/sec$ $\Delta G_{Cd} = -0.530ev$
$D_{s(Pb)} = 1.90 \times 10^{-09}\ cm^2/sec$ $\Delta G_{Pb} = -0.400ev$

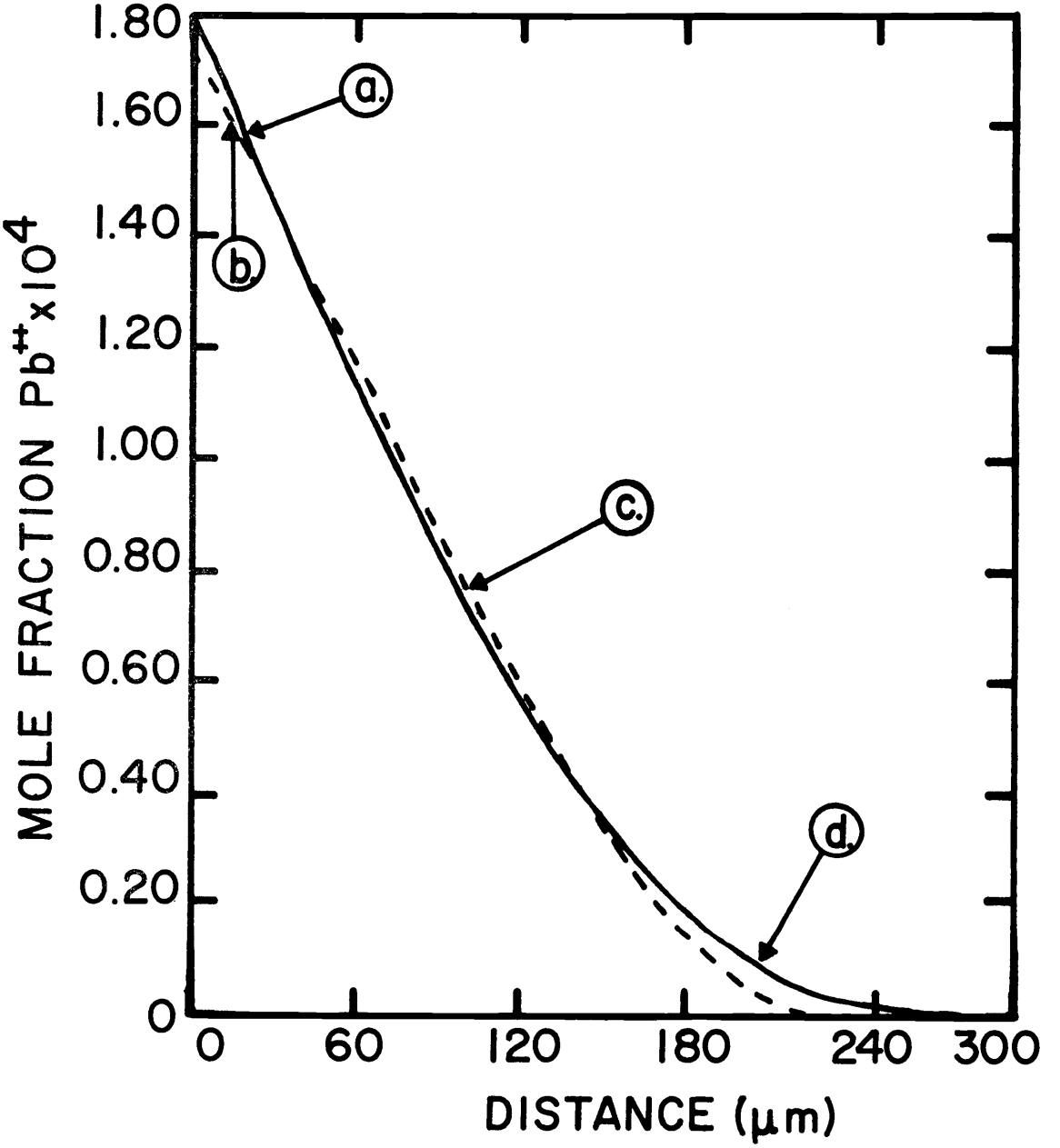

Figure 5.8. Trial profiles used in determining correct parameters to fit Pb^{++} profiles in KCl. Sections c. and d. of the profiles are important. Curve a. is profile used to fit the experimental data in Figure (5.4). T = 492°C, $t_t = 8.600 \times 10^5$ sec.

a. $D_{s(Cd)} = 8.10 \times 10^{-09} cm^2/sec$ $\Delta G_{Cd} = -0.565 ev$
$D_{s(Pb)} = 1.15 \times 10^{-09} cm^2/sec$ $\Delta G_{Pb} = -0.500 ev$

b. $D_{s(Cd)} = 8.00 \times 10^{-09} cm^2/sec$ $\Delta G_{Cd} = -0.600 ev$
$D_{s(Pb)} = 1.90 \times 10^{-09} cm^2/sec$ $\Delta G_{Pb} = -0.400 ev$

Cd^{++} profile can be determined without separating the Cd^{++} from the Pb^{++}. Therefore, three experiments, which did not have the Cd^{++} separated, are used, but the calculated profile may not fit the experimental one near the surface since the measured concentrations in this region may not be correct. The experiments, in which the Cd^{++} is separated, show that the unusual profiles are real and that the generated profiles agree very well with these profiles.

The insensitivity of a major section of the diffusion profile, once it has become well established, to the boundary conditions was investigated by an experiment in which the Pb^{++} and Cd^{++} were desorbed from crystal B of the diffusion anneal at 458 °C, Figure (5.3). After its initial anneal, crystal B was placed in an evacuated ampoule which contained no diffusants, and it was again annealed for a known period of time. The ideal boundary conditions would be

$$c = 0 \quad \text{at} \quad x = 0, \quad t > 0, \tag{5.2}$$

but experimentally this would not be true since as the cations were desorbed, the vapor pressure would increase in the ampoule to approximately 10^{-2}-10^{-3} torr, and the surface concentration would not be zero. Qualitative evidence for this is the profiles in Figure (5.9). The generated profiles, while naturally not fitting the profiles near the surface, agree very well with the major sections.

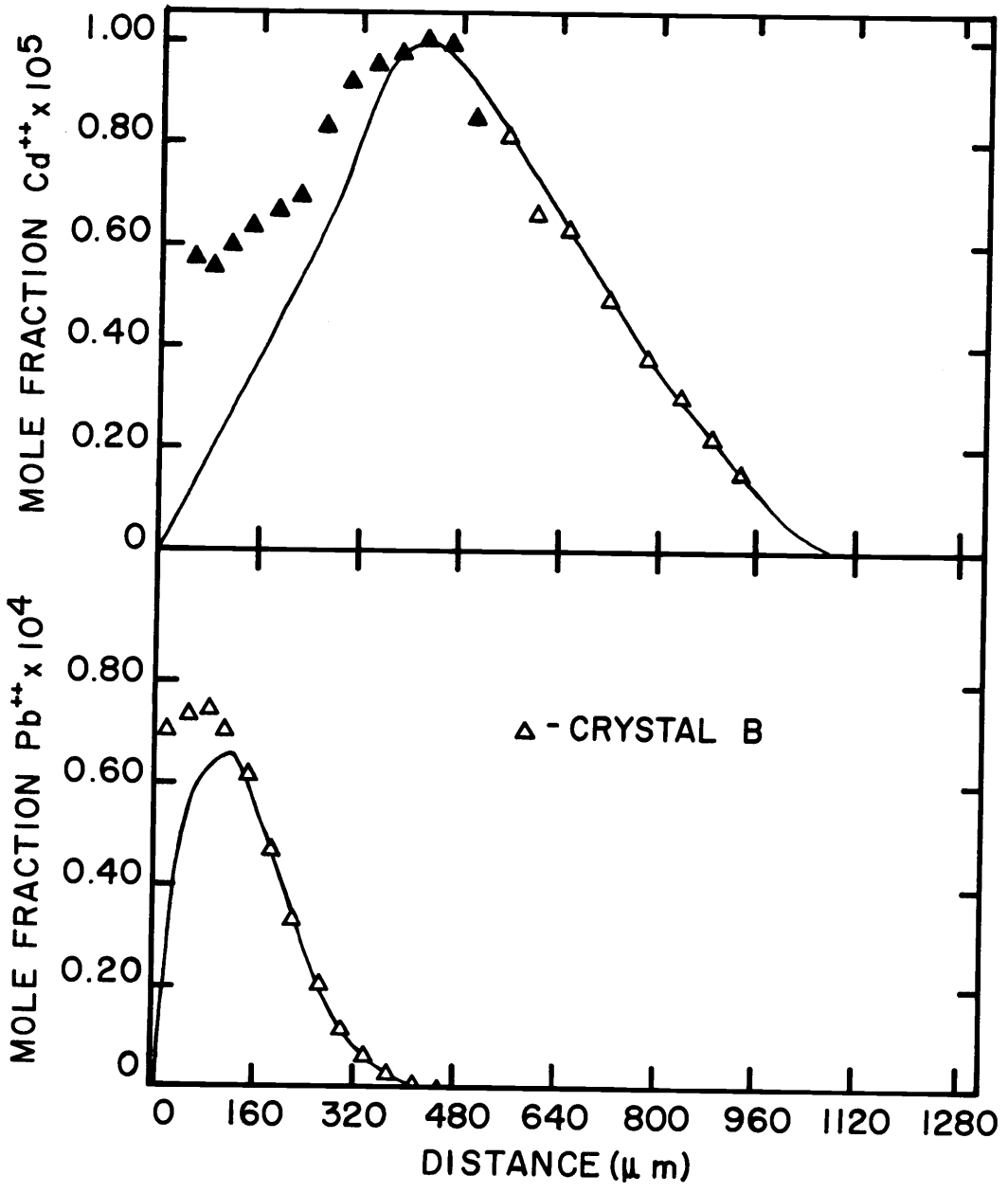

Figure 5.9. Penetration profiles for the desorption of cadmium and lead ions from crystal B of the same experiment as crystal A, Figure (5.2). $T = 450^{\circ}C$. $t_t = 8.920 \times 10^4$ sec. Filled in symbols represent separated Cd^{++}. Solid curves are profiles generated by finite differences using the following parameters.

$D_{s(Cd)} = 5.70 \times 10^{-09} cm^2/sec \quad \Delta G_{Cd} = -0.563ev$

$D_{s(Pb)} = 5.40 \times 10^{-10} cm^2/sec \quad \Delta G_{Pb} = -0.495ev$

Figure (5.10) shows plots of $\log_{10} D_s$ versus $1/T$. The solid lines are found by a least squares analysis and are described by

$$D_{s(Pb)} = 1.00 \times 10^{-3} \exp(-0.908 ev/kT) \ cm^2/sec \qquad (5.3)$$

and

$$D_{s(Cd)} = 4.05 \times 10^{-5} \exp(-0.557 ev/kT) \ cm^2/sec. \qquad (5.4)$$

Where 0.908 ev is the activation energy of migration of the Pb^{++}-vacancy complex, and 0.557 ev is that of the Cd^{++}-vacancy complex.

The thermodynamic functions, ΔH (enthalpy) and ΔS^1 (entropy), are calculated from the following expression.

$$\Delta G = \Delta H - T\Delta S^1 \qquad (5.5)$$

It is emphasized that ΔS^1 is the entropy of formation excluding the configurational entropy. Plots of ΔG versus T are given in Figure (5.11). The following expressions give the calculated change of the Gibbs free energy with temperature.

$$\Delta G_{Pb} = -0.378 ev - (1.604 \times 10^{-4} \ ev/°K) \ T \qquad (5.6)$$

$$\Delta G_{Cd} = -0.474 ev - (1.230 \times 10^{-4} \ ev/°K) \ T \qquad (5.7)$$

Where -0.378 ev and -0.474 ev are enthalpies of formation of the Pb^{++}-vacancy complex and the Cd^{++}-vacancy complex, respectively.

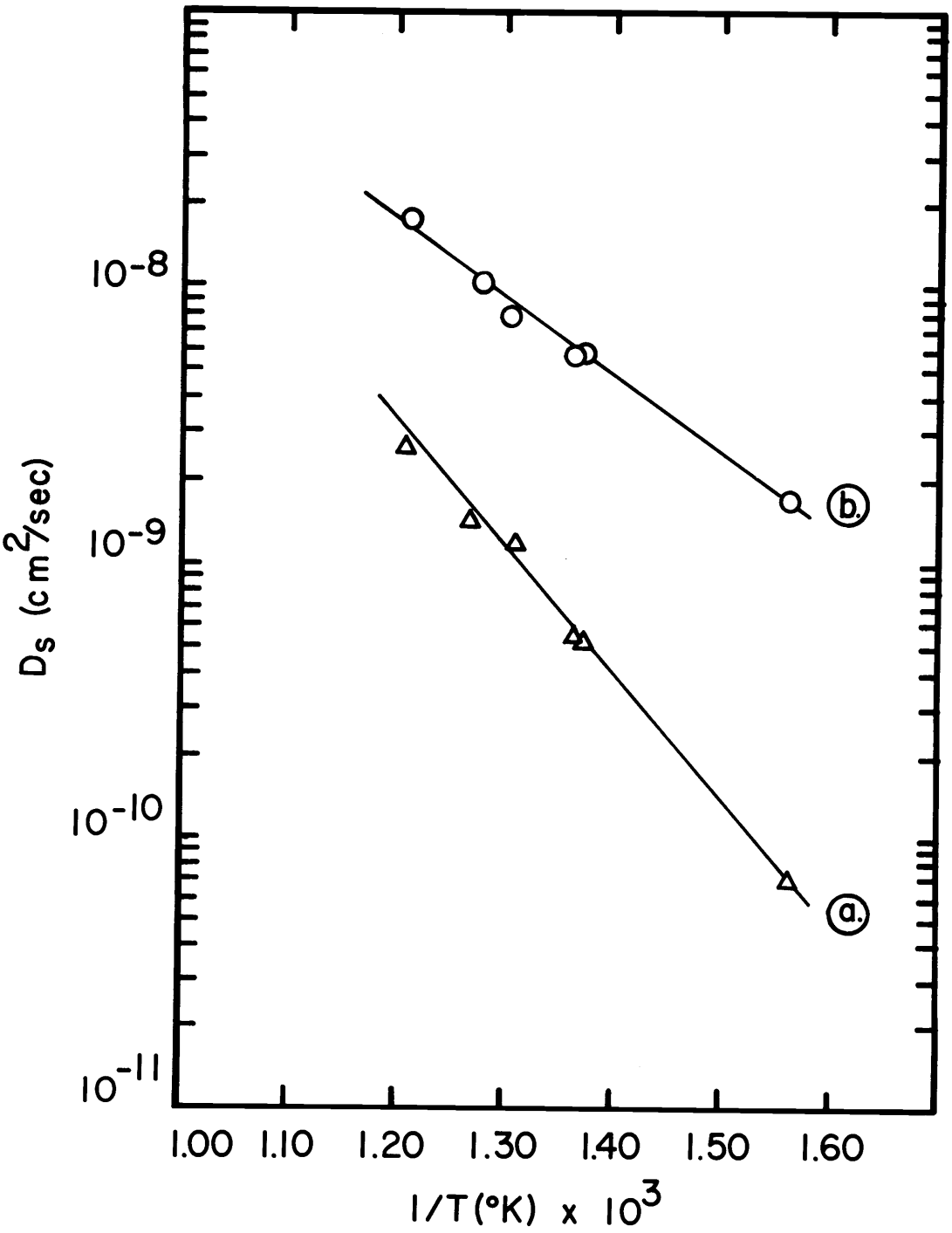

Figure 5.10. Log D_s vs. 1/T from diffusion in KCl. The Pb^{++} results are fit by line a. and those of Cd^{++} by line b.

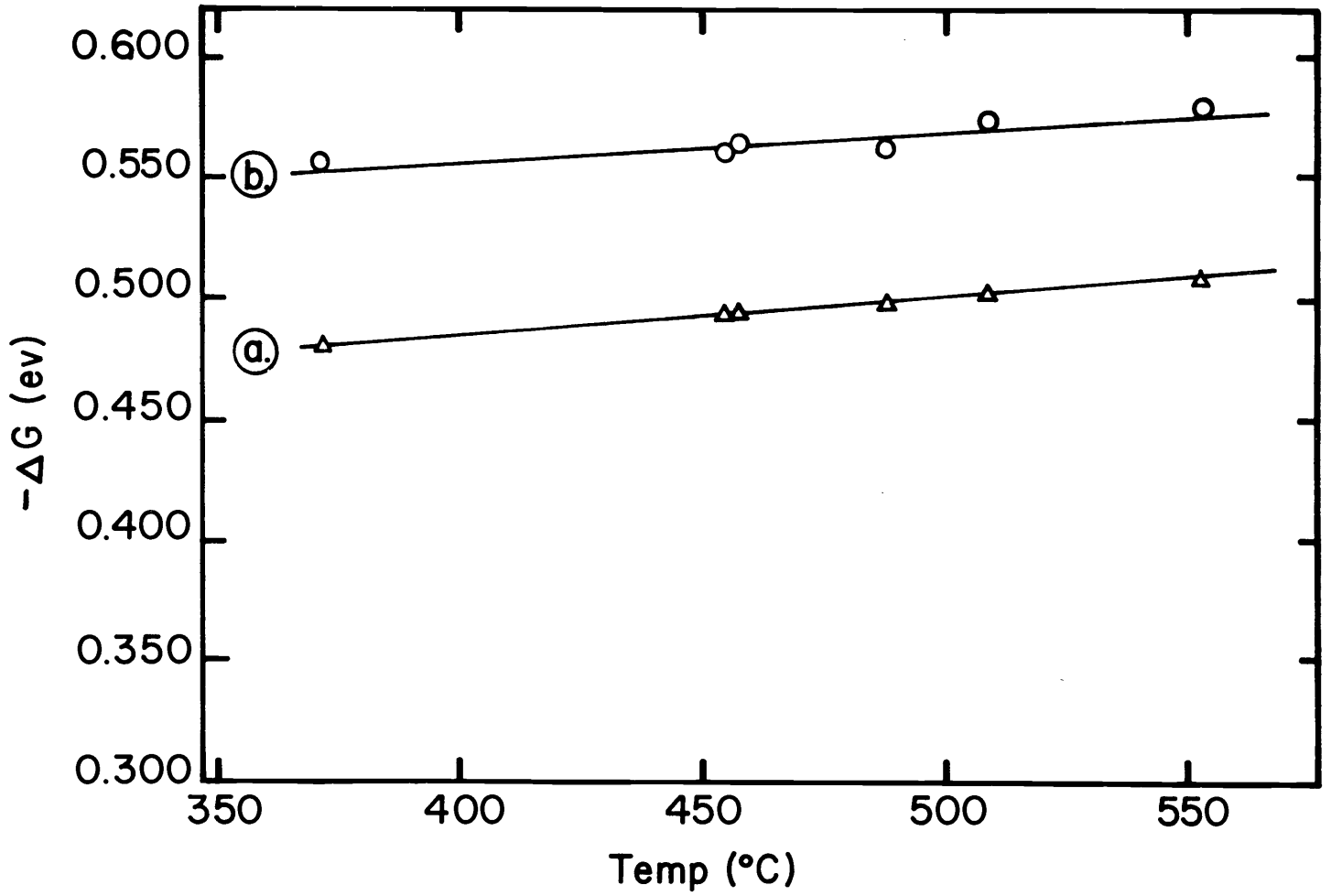

Figure 5.11. Gibbs free energies of association of impurity-vacancy complexes in NaCl. The Pb^{++} results are fit by line a. and those of Cd^{++} by line b.

The entropies of formation of these complexes are 1.604×10^{-4} ev/°K for the lead complex and 1.230×10^{-4} ev/°K for the cadmium complex.

Sodium Chloride

Profiles of the diffusion of Pb^{++} and Cd^{++} in NaCl, which show the fit of the calculated profiles to the experimental ones, are shown in Figures (5.12) through (5.20). The values of the parameters used for the calculated profiles are listed in Table (5.2). In NaCl the thermal vacancies were considered negligible since the concentrations of both diffusants were more than an order of magnitude greater than the calculated thermal vacancies in a pure crystal (9). Since the experimental profiles, which were from experiments where the cooling coil was not used, could be fit by using reasonable parameters except near the surface, they were satisfactory for calculation of diffusion parameters.

The desorption of the diffusants during quenching was investigated, as a possible cause of the misfit of the profiles near the surface, by generating desorption profiles from the calculated profiles as indicated in Figure (5.21). The values of the temperature and diffusion coefficients are varying in a complex manner during this quenching period, and the constant parameters used in calculating the desorption profiles represent optimum conditions of desorption. It

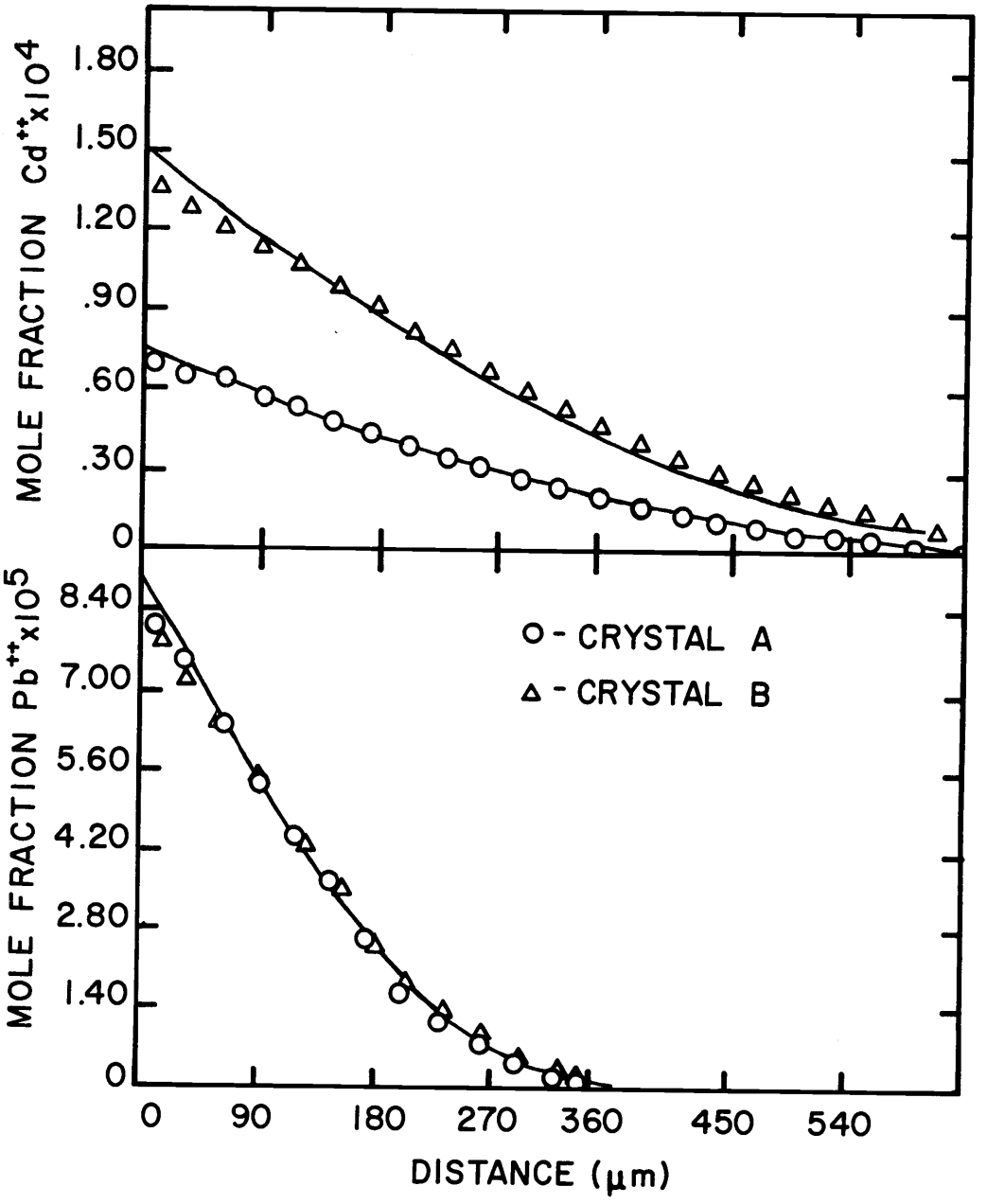

Figure 5.12. Penetration profiles for the diffusion of cadmium and lead ions in NaCl at 347°C. $t_t = 1.1239 \times 10^5$ sec. Air quenched. Solid curves are profiles generated by finite differences using the following parameters.

a. $D_{s(Cd)} = 4.10 \times 10^{-10}$ cm^2/sec $\quad \Delta G_{Cd} = -0.560$ev

b. $D_{s(Cd)} = 4.50 \times 10^{-10}$ cm^2/sec $\quad \Delta G_{Cd} = -0.560$ev

a, b. $D_{s(Pb)} = 1.70 \times 10^{-10}$ cm^2/sec $\quad \Delta G_{Pb} = -0.445$ev

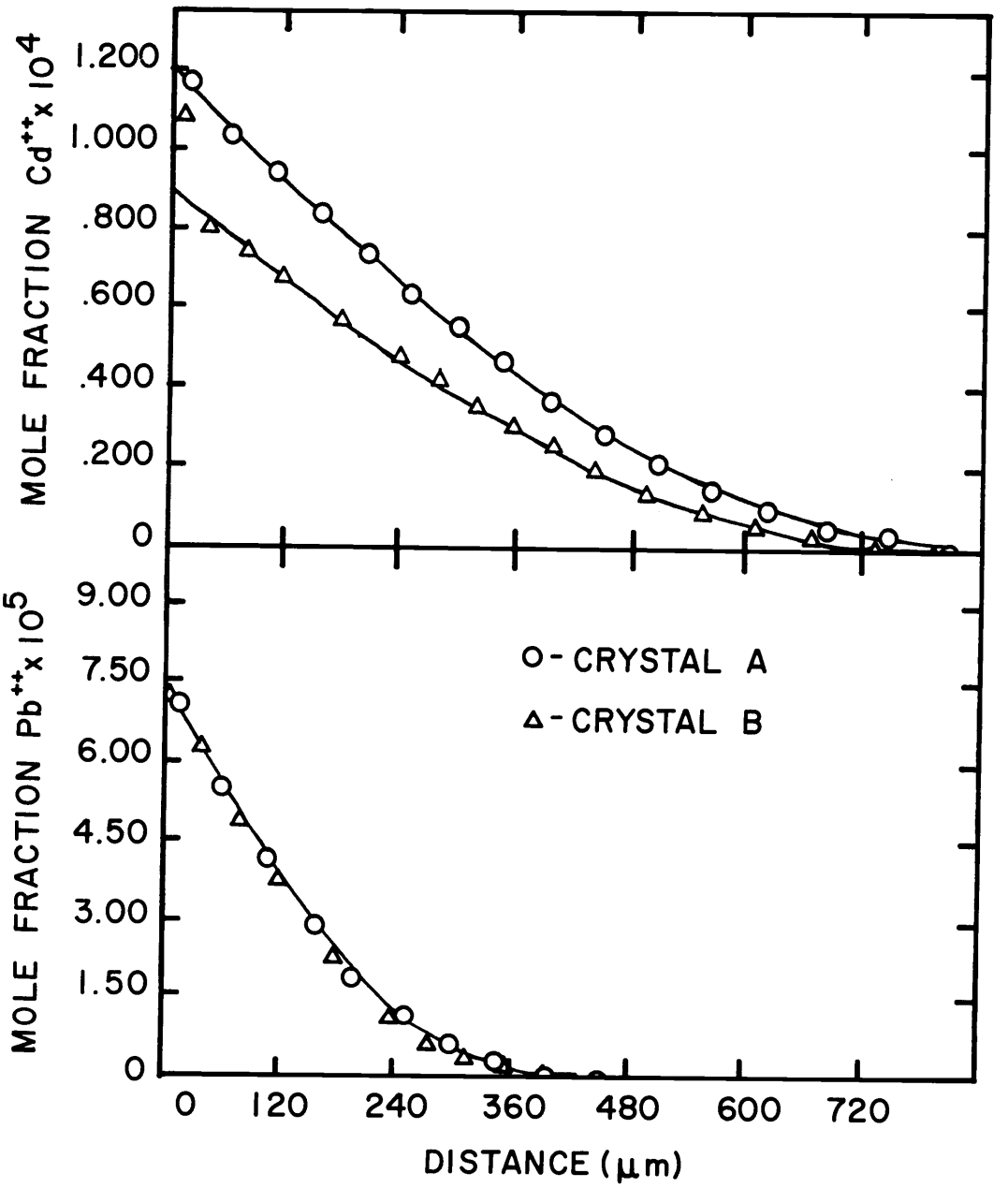

Figure 5.13. Penetration profiles for the diffusion of cadmium and lead ions in NaCl at 360°C. $t_t = 1.2890 \times 10^6$ sec. Liquid quenched. Solid curves are profiles generated by finite differences using the following parameters.

a. $D_{s(Cd)} = 5.80 \times 10^{-10}$ cm^2/sec $\quad \Delta G_{Cd} = -0.550$ev

b. $D_{s(Cd)} = 5.00 \times 10^{-10}$ cm^2/sec $\quad \Delta G_{Cd} = -0.550$ev

a, b. $D_{s(Pb)} = 1.90 \times 10^{-10}$ cm^2/sec $\quad \Delta G_{Pb} = -0.440$ev

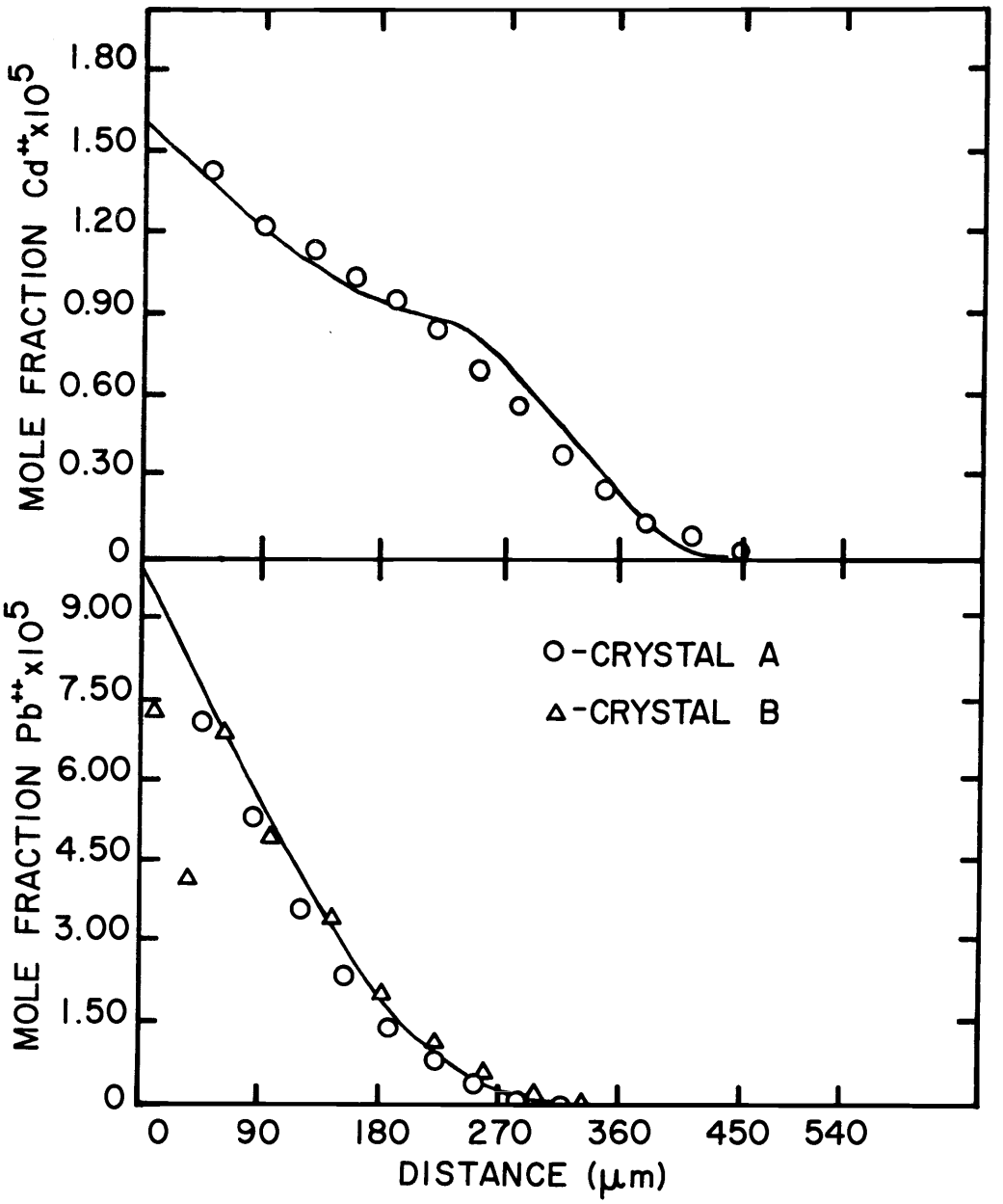

Figure 5.14. Penetration profiles for the diffusion of cadmium and lead ions in NaCl at 409°C. $t_t = 2.451 \times 10^5$ sec. Liquid quenched. Solid curves are profiles generated by finite differences using the following parameters.

$D_{s(Cd)} = 1.60 \times 10^{-09}$ cm^2/sec $\quad \Delta G_{Cd} = -0.520$ev

$D_{s(Pb)} = 7.60 \times 10^{-10}$ cm^2/sec $\quad \Delta G_{Pb} = -0.440$ev

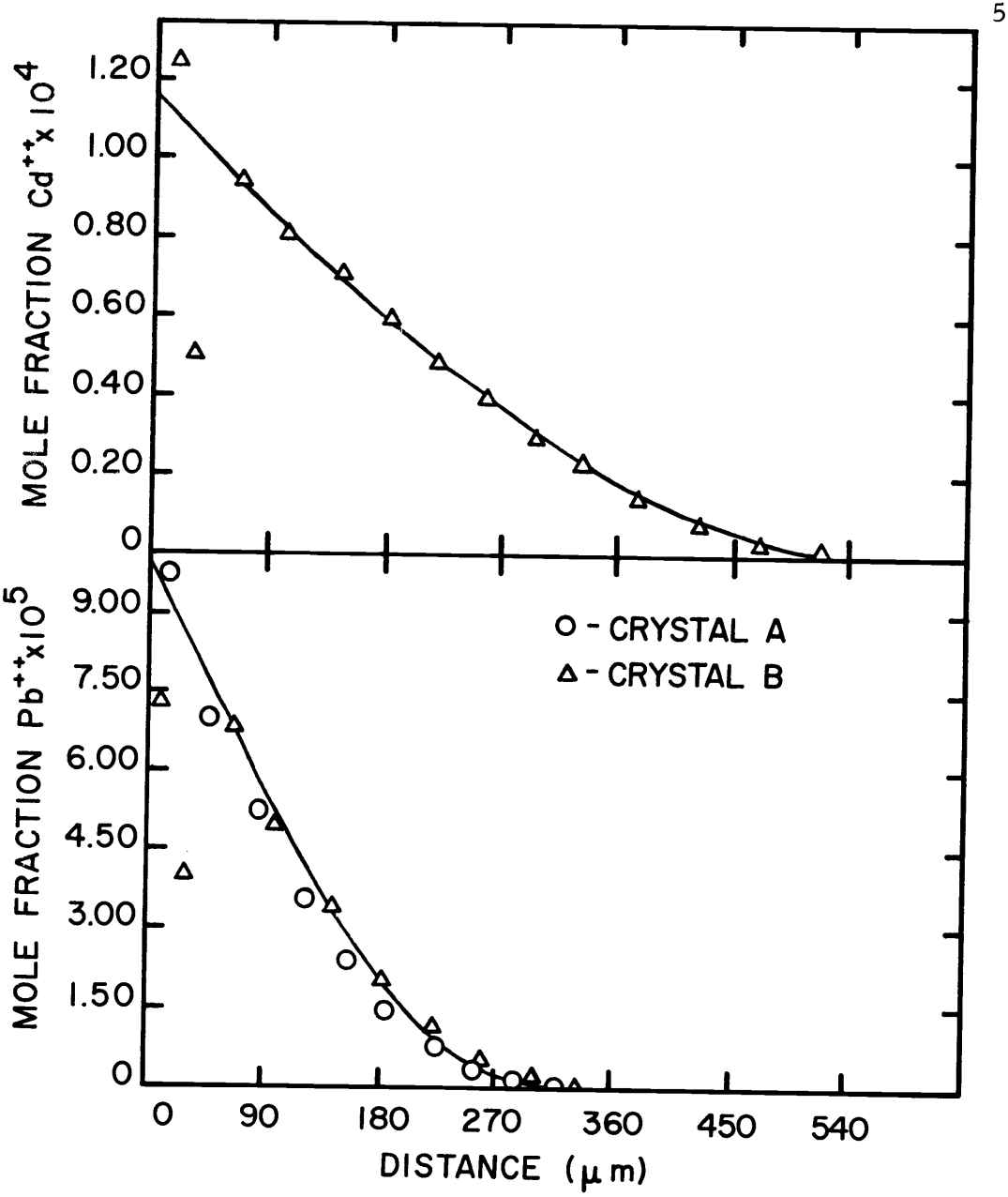

Figure 5.15. Penetration profiles for the diffusion of cadmium and lead ions in NaCl at 409°C. $t_t = 2.451 \times 10^5$sec. Liquid quenched. Solid curves are profiles generated by finite differences using the following parameters.

$D_{s(Cd)} = 1.45 \times 10^{-09} cm^2/sec \quad \Delta G_{Cd} = -0.520ev$

$D_{s(Pb)} = 7.60 \times 10^{-09} cm^2/sec \quad \Delta G_{Pb} = -0.415ev$

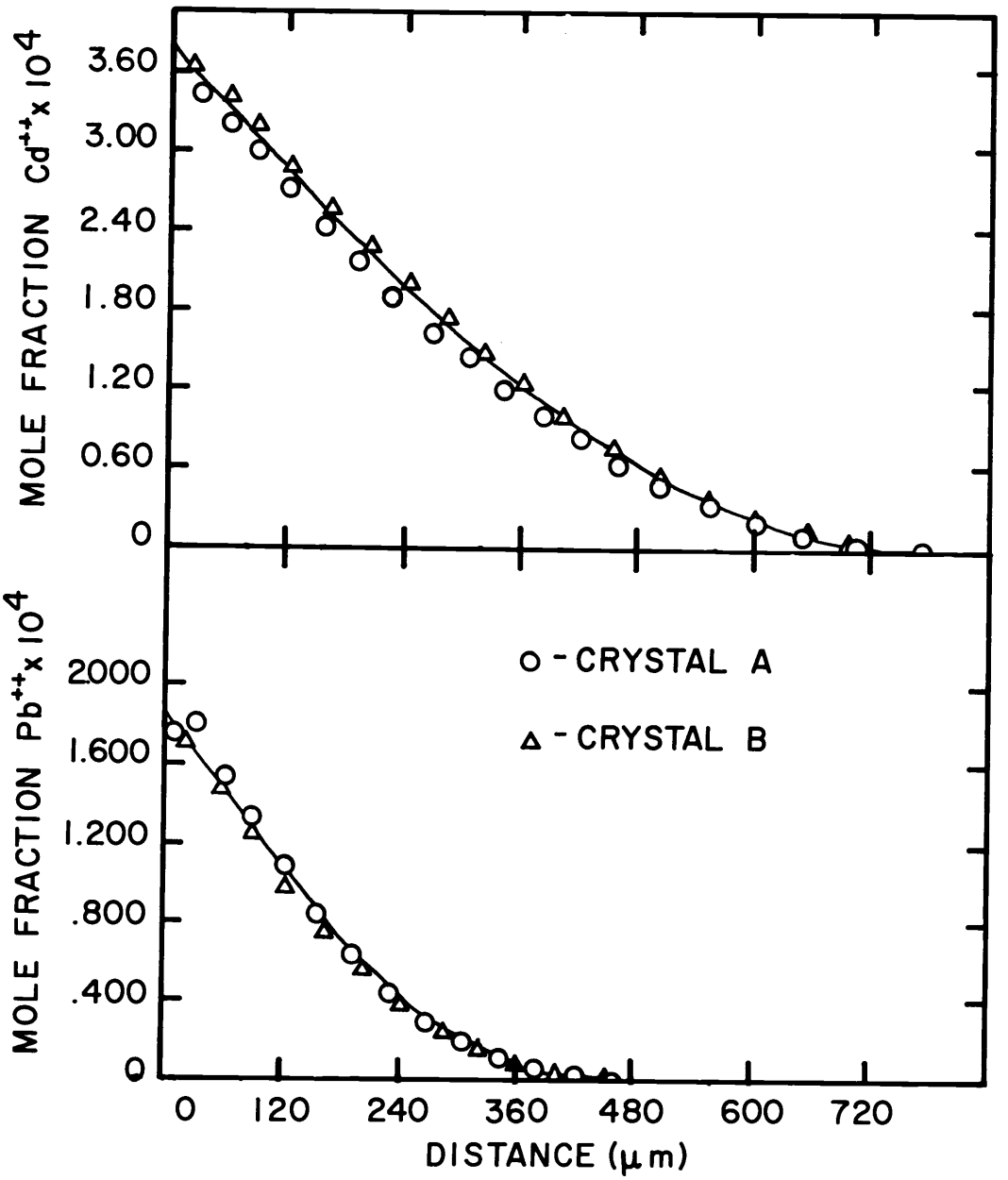

Figure 5.16. Penetration profiles for the diffusion of cadmium and lead ions in NaCl at 460°C. $t_t = 1.674 \times 10^5$ sec. Liquid quenched. Solid curves are profiles generated by finite differences using the following parameters.

$D_{s(Cd)} = 4.10 \times 10^{-09}$ cm^2/sec $\quad \Delta G_{Cd} = -0.485$ev

$D_{s(Pb)} = 2.30 \times 10^{-09}$ cm^2/sec $\quad \Delta G_{Pb} = -0.388$ev

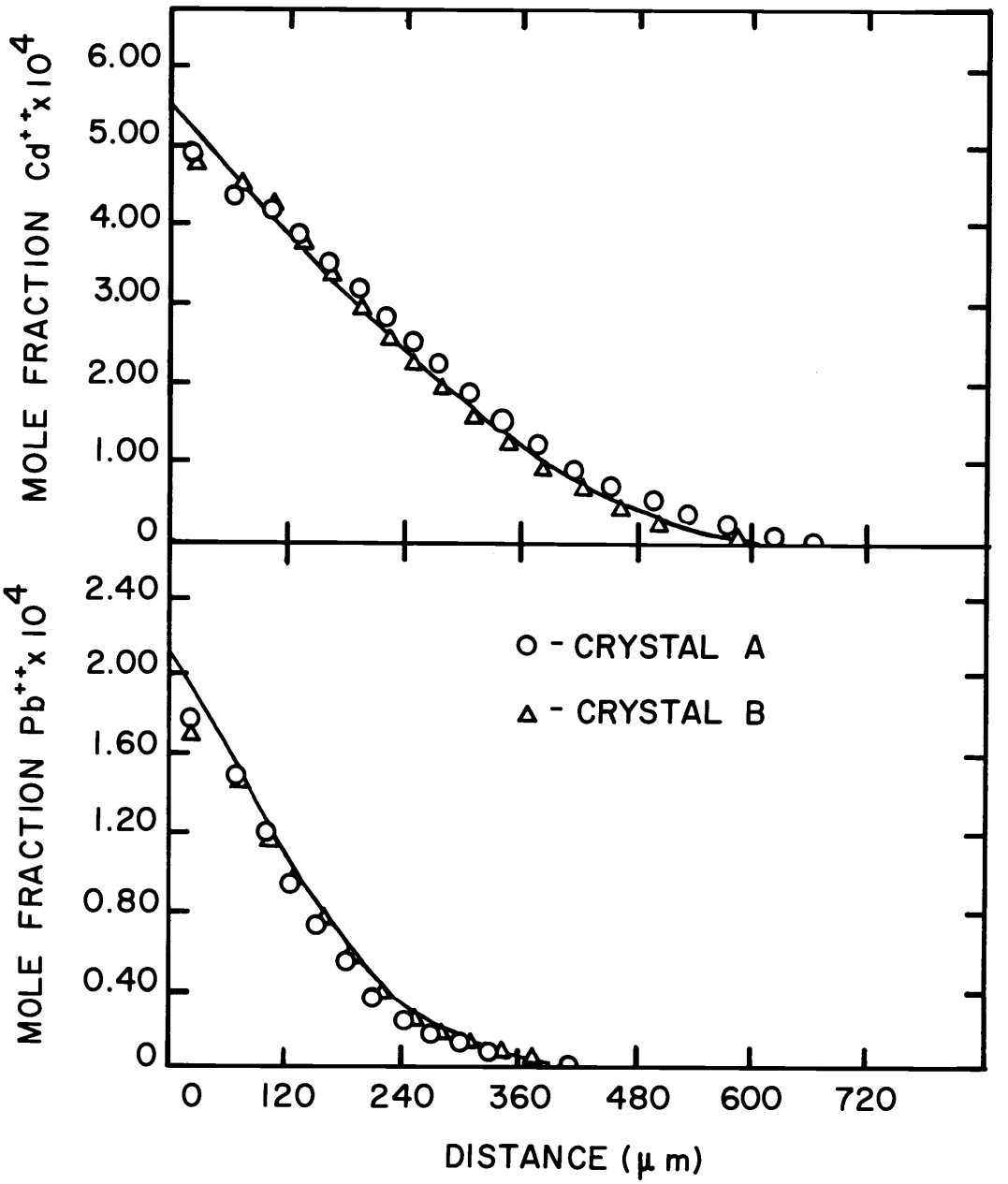

Figure 5.17. Penetration profiles for the diffusion of cadmium and lead ions in NaCl at 497°C. $t_t = 6.730 \times 10^4$ sec. Liquid quenched. Solid curves are profiles generated by finite differences using the following parameters.

$D_{s(Cd)} = 7.50 \times 10^{-09}$ cm^2/sec $\quad \Delta G_{Cd} = -0.455$ev

$D_{s(Pb)} = 4.60 \times 10^{-09}$ cm^2/sec $\quad \Delta G_{Pb} = -0.370$ev

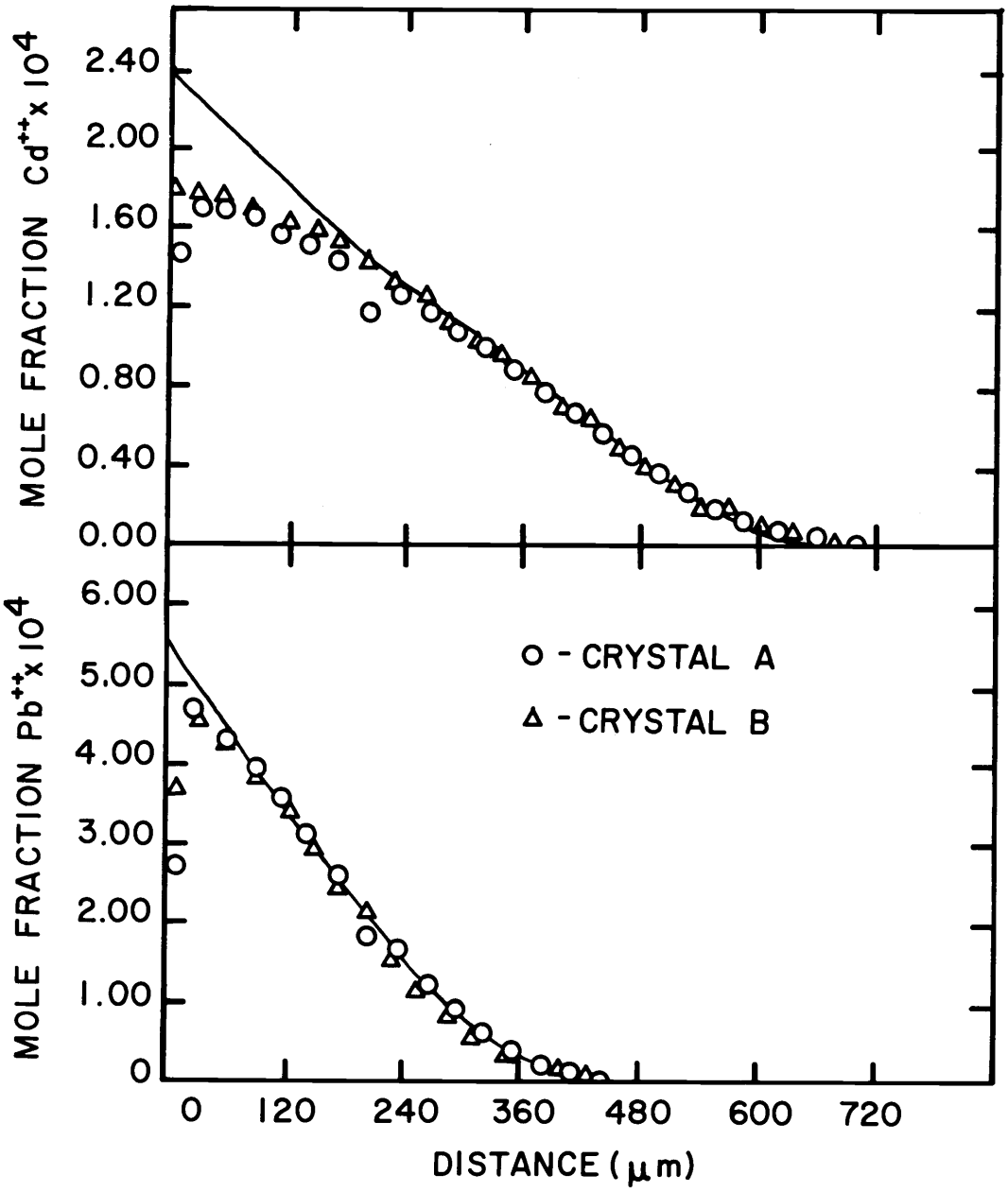

Figure 5.18. Penetration profiles for the diffusion of cadmium and lead ions in NaCl at 502°C. $t_t = 7.200 \times 10^4$sec. Air quenched. Solid curves are profiles generated by finite differences using the following parameters.

$D_{s(Cd)} = 1.00 \times 10^{-08}$ cm^2/sec $\quad \Delta G_{Cd} = -0.453$ev

$D_{s(Pb)} = 5.80 \times 10^{-09}$ cm^2/sec $\quad \Delta G_{Pb} = -0.367$ev

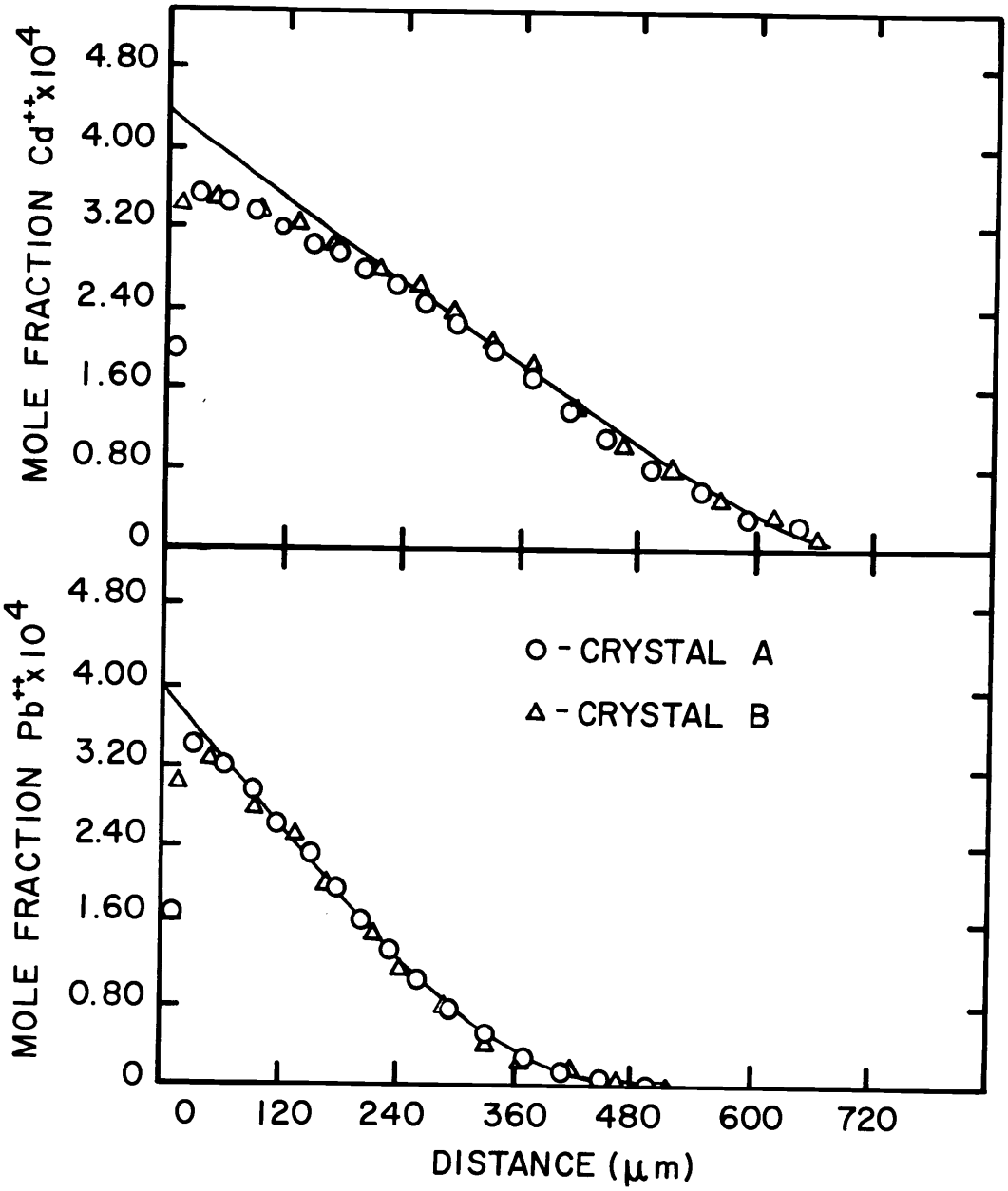

Figure 5.19. Penetration profiles for the diffusion of cadmium and lead ions in NaCl at 553°C. $t_t = 4.368 \times 10^4$ sec. Liquid quenched. Solid curves are profiles generated by finite differences using the following parameters.

$D_{s(Cd)} = 2.40 \times 10^{-08}$ cm^2/sec $\quad \Delta G_{Cd} = -0.424$ev

$D_{s(Pb)} = 1.50 \times 10^{-08}$ cm^2/sec $\quad \Delta G_{Pb} = -0.342$ev

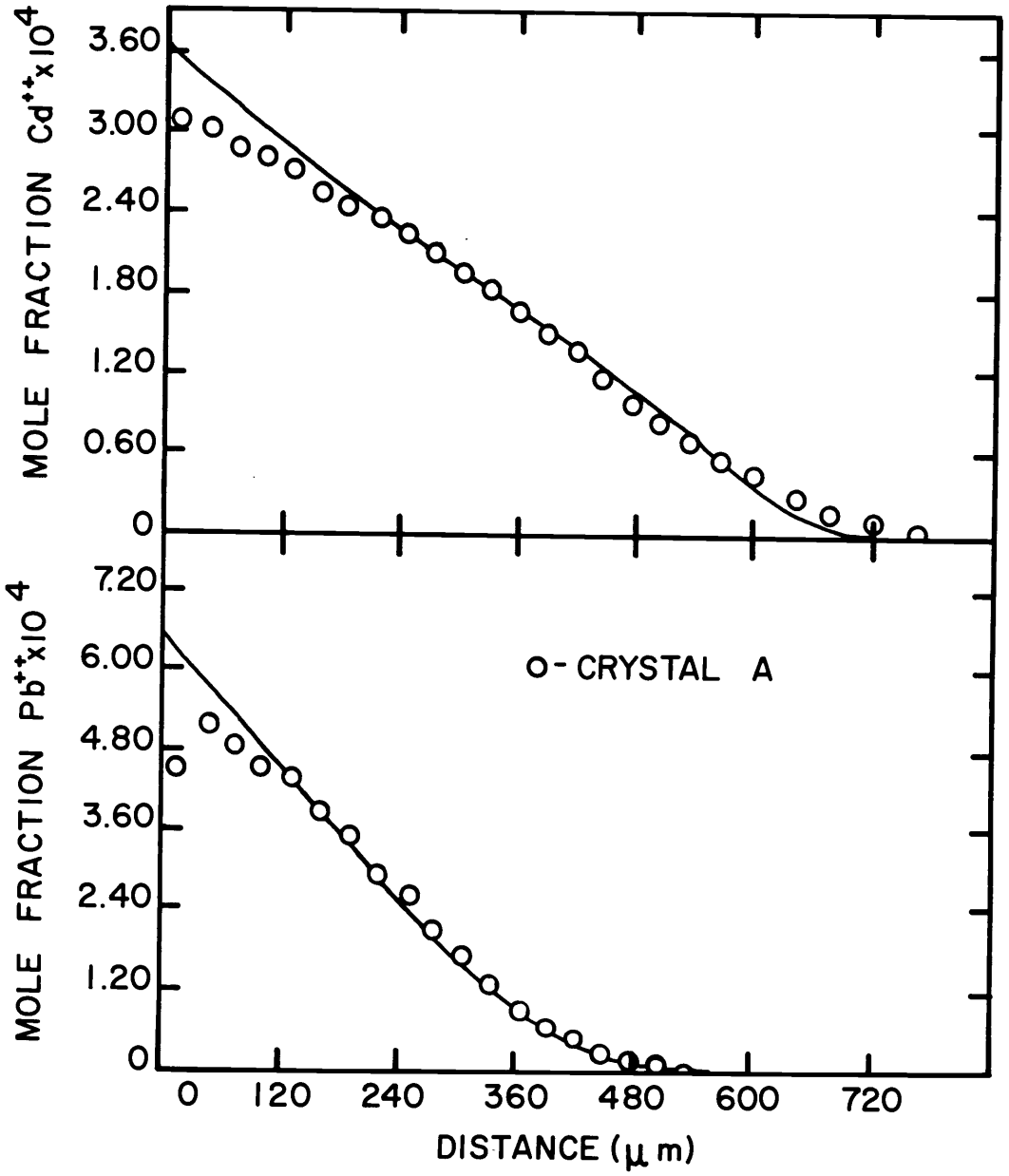

Figure 5.20. Penetration profiles for the diffusion of cadmium and lead ions in NaCl at 569°C. $t_t = 4.212 \times 10^4$ sec. Air quenched. Solid curves are profiles generated by finite differences using the following parameters.

$D_{s(Cd)} = 2.75 \times 10^{-08}$ cm^2/sec $\quad \Delta G_{Cd} = -0.414$ev

$D_{s(Pb)} = 2.00 \times 10^{-08}$ cm^2/sec $\quad \Delta G_{Pb} = -0.323$ev

Table 5.2. Values of D_s and ΔG used to generate diffusion profiles of Pb^{++} and Cd^{++} in NaCl.

T (°C)	$D_{s(Pb)}$ (cm^2/sec)	$D_{s(Cd)}$ (cm^2/sec)	ΔG_{Pb} (ev)	ΔG_{Cd} (ev)	Notes
347	1.70×10^{-10}	4.10×10^{-10}	-0.445	-0.560	a, d
347	1.70×10^{-10}	4.50×10^{-10}	-0.445	-0.560	b, d
360	1.90×10^{-10}	5.80×10^{-10}	-0.440	-0.550	a, c
360	1.90×10^{-10}	5.00×10^{-10}	-0.440	-0.550	b, c
409	7.60×10^{-10}	1.60×10^{-09}	-0.415	-0.520	a, c
409	7.60×10^{-10}	1.45×10^{-09}	-0.415	-0.520	b, c
460	2.30×10^{-09}	4.10×10^{-09}	-0.388	-0.485	a, b, c
497	4.60×10^{-09}	7.50×10^{-09}	-0.370	-0.455	a, b, c
502	5.80×10^{-09}	1.00×10^{-08}	-0.367	-0.453	a, b, d
553	1.50×10^{-08}	2.40×10^{-08}	-0.342	-0.424	a, b, c
569	2.00×10^{-08}	2.75×10^{-08}	-0.323	-0.414	a, d

a. Crystal A
b. Crystal B
c. Cooling coil used, crystal quenched after diffusion anneal.
d. No cooling coil used, crystal air quenched.

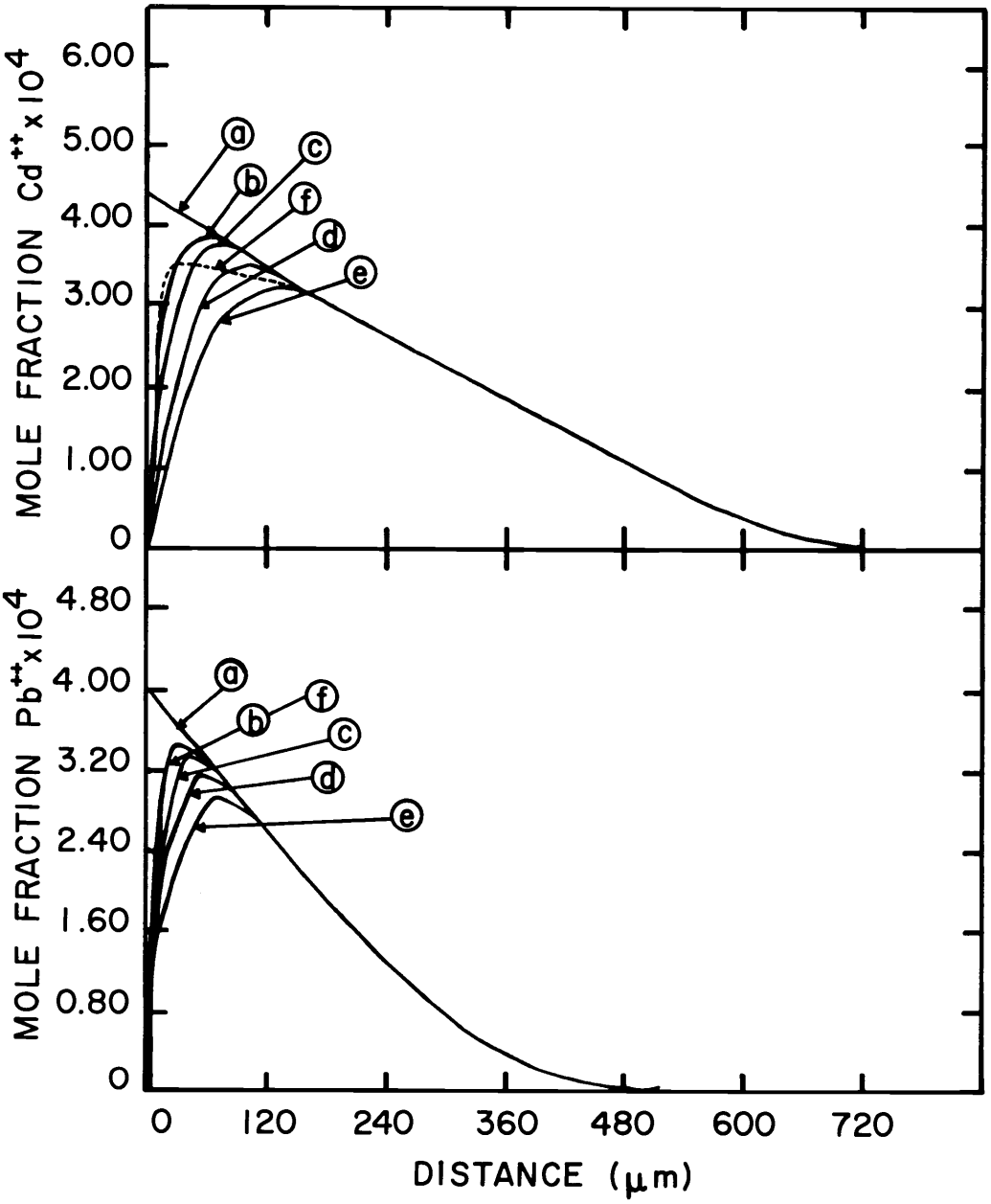

Figure 5.21. Penetration profiles for the desorption of cadmium and lead from NaCl at 553°C for short periods of time. Calculated by finite differences using the following parameters.

$D_{s(Cd)} = 2.40 \times 10^{-08} cm^2/sec \quad \Delta G_{Cd} = -0.424ev$

$D_{s(Pb)} = 1.50 \times 10^{-08} cm^2/sec \quad \Delta G_{Pb} = -0.342ev$

a. 0 min b. 2 min c. 4 min d. 10 min

e. 20 min f. average of experimental points.

appears that a major portion of the surface anomaly in NaCl can be explained by this desorptive process. Since the diffusion parameters in KCl are similar to those in NaCl at the higher temperatures, this desorptive process would also be operative in the KCl crystals.

Plots of $\log_{10} D_s$ versus $1/T$ are illustrated in Figure (5.22). $D_{s(Pb)}$ and $D_{s(Cd)}$ are found to be represented by

$$D_{s(Pb)} = 1.40 \times 10^{-2} \exp(-0.982 ev/kT) \text{ cm}^2/\text{sec} \qquad (5.8)$$

and

$$D_{s(Cd)} = 3.57 \times 10^{-3} \exp(-0.857 ev/kT) \text{ cm}^2/\text{sec}. \qquad (5.9)$$

Where the activation energy of migration of the Pb^{++}-vacancy complex is 0.982 ev, and that of the Cd^{++}-vacancy complex is 0.857 ev. The Gibbs free energies of association of the two complexes are expressed by

$$\Delta G_{Pb} = -0.775 ev + (5.29 \times 10^{-4} ev/°K)\ T \qquad (5.10)$$

and

$$\Delta G_{Cd} = -0.972 ev + (6.65 \times 10^{-4} ev/°K)\ T. \qquad (5.11)$$

The enthalpy and entropy of formation for the lead complex are -0.775 ev and -5.29×10^{-4} ev/°K respectively, and the values of the same functions for the cadmium complex are -0.972 ev and -6.65×10^{-4} ev/°K. Plots of ΔG versus T are shown in

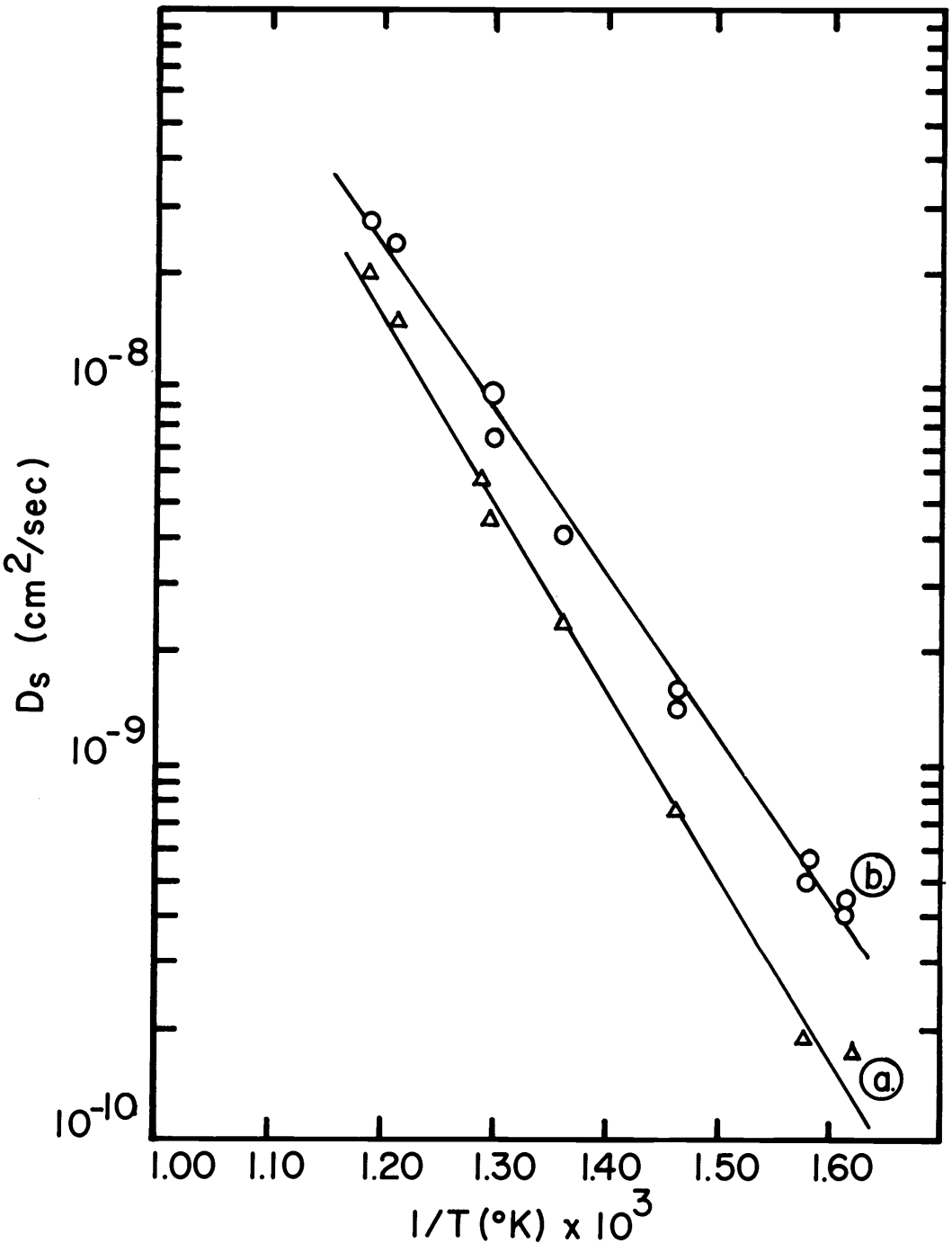

Figure 5.22. Log D_s vs. 1/T from diffusion in NaCl. The Pb^{++} results are fit by line a. and those of Cd^{++} by line b.

Figure (5.23).

It is very difficult to quantitatively, or even qualitatively, define the limits of errors in diffusion work. The concentration and weights of the individual samples are mostly accurate to ±3%, except for the concentrations determined by chemical separation, which probably fall within ±5% of the correct values. With the exception of the sections near the surface, which have been discussed, the calculated curves fit the experimental profiles within the above experimental errors. Therefore, the parameters calculated are valid within ±5%.

The raw data necessary for the calculation of the experimental profiles is given in Appendix I.

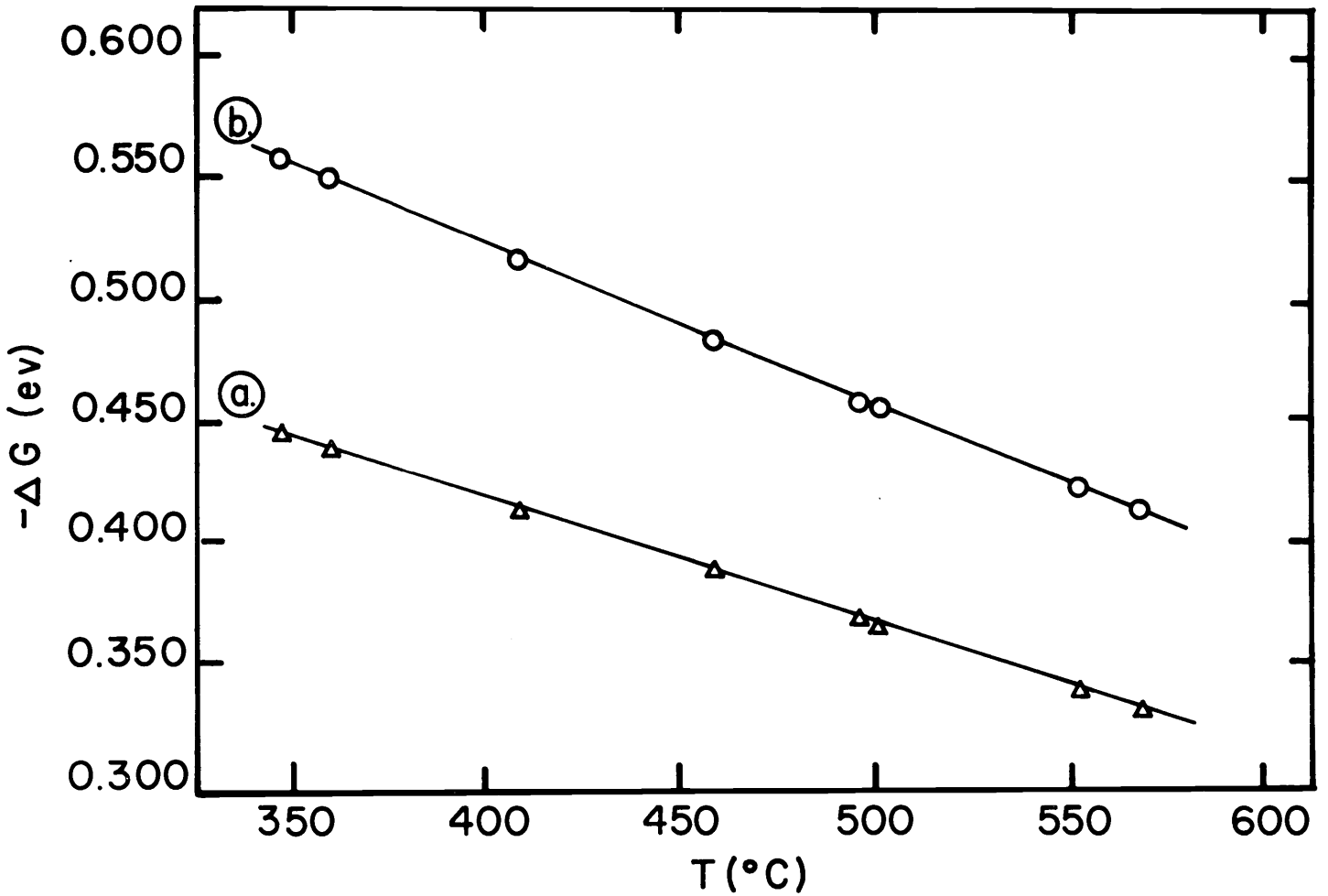

Figure 5.23. Gibbs free energies of association of impurity-vacancy complexes in KCl. The Pb^{++} results are fit by line a. and those of Cd^{++} by line b.

VI. DISCUSSION

Mannion, Allen and Fredericks (28) have studied the diffusion of Pb^{++} in purified NaCl. Of the systems studied in this work, this has been the only investigation of diffusion in crystals grown from the ion-exchange salts. Results of the Pb^{++}-vacancy complex diffusion in NaCl agree very well with this earlier work as shown in Table (6.1).

The other results are compared to diffusion studies of divalent cations in Harshaw Chemical Company single crystals. These are also compared in Table (6.1). Harshaw crystals are known to contain a higher concentration of divalent cations than the purified crystals used in this study, and also, the commercial crystals contain a much higher concentration of OH^- since they are grown in air.

It is found that the values of the Gibbs free energies of association are generally larger than those measured when the commercial crystals were used. The opposite would be expected if only the unintentional divalent cations were considered, as shown in the work by Allen, Ireland, and Fredericks (3) and by Mannion et al. Therefore, the possible effects of OH^- must be discussed.

Fritz, Luty and Anger (13) have reported a reaction of Ca^{++} with OH^- in KCl single crystals. Allen (1, p. 90-122) has found the OH^- impurity in KCl has a strong effect on the diffusion of Hg^{++}.

Table 6.1. Values of D_o, the migration energy U_o, the enthalpy of formation and the entropy[b] of formation of the Pb^{++} and Cd^{++} complexes in NaCl and KCl.

Crystal	Cation	[a] D_o (cm^2/sec)	[a] U_o (ev)	[b] ΔH (ev)	[b] ΔS^1 (ev/°K)	Reference
[d] NaCl	Pb^{++}	1.75×10^{-2}	0.98	-0.780	-5.31×10^{-4}	28
[d] NaCl	Pb^{++}	1.40×10^{-2}	0.982	-0.775	-5.29×10^{-4}	This work
[c] NaCl	Pb^{++}	1.5×10^{-2}	0.99	-0.632	-2.60×10^{-4}	3
[c] NaCl	Cd^{++}	2.06×10^{-2}	0.92	-1.085	-8.95×10^{-4}	2
[d] NaCl	Cd^{++}	3.57×10^{-3}	0.857	-0.972	-6.65×10^{-4}	This work
[c] KCl	Pb^{++}	1.1×10^{-2}	1.18	-1.188	-1.00×10^{-3}	23
[d] KCl	Pb^{++}	1.00×10^{-3}	0.908	-0.378	$+1.60 \times 10^{-4}$	This work
[c] KCl	Cd^{++}	4.68×10^{-5}	0.54	-0.412	$+1.39 \times 10^{-4}$	20
[d] KCl	Cd^{++}	4.05×10^{-5}	0.557	-0.474	$+1.23 \times 10^{-4}$	This work

a. $D_s = D_o \exp(-U_o/kT)$

b. $\Delta G = \Delta H - T\Delta S^1$, ΔS^1 is the entropy excluding the configurational entropy.

c. Harshaw crystals

d. Crystals grown from ion-exchange purified salt.

The exact products of the reaction of the divalent cation with OH^- are not known, but that the reaction is essentially complete is evidenced in both of these studies.

A reason that OH^- should affect the results of most divalent cation diffusion studies is that, if the OH^- reacts with the divalent cations, the reaction product will trap the divalent cation. Another way of looking at the effect of OH^- is that another reaction is competing for the divalent cation in the association reaction

$$M^{++} + V_c^- \rightleftharpoons MV_c^+ . \qquad (6.1)$$

If this competition is ignored, the value of the Gibbs free energy observed in this case will be smaller than its true value.

The formation of a partially covalent bond between OH^- and the divalent cation seems to be a prime reason why OH^- should behave differently than Cl^-. One case, in which the OH^- may not affect the diffusion results of a divalent cation, is when the divalent cation is considerably larger than the host cation it has replaced. The lattice and the electron cloud of the divalent cation are already severely distorted, and any partial transfer of electrons to the cation from the OH^- would only cause greater distortion. Mannion's et al. and Allen's et al. studies of Pb^{++} diffusion in NaCl support this argument.

Some insight into D_s and its temperature dependence can

be gained by considering a special case. If the concentration of the cation vacancies is much greater than that of the divalent cations and is constant, the diffusion coefficient will be constant. According to Lidiard (25, p. 338), it can be expressed as

$$D_T = D_s p = a_o^2 \omega_2 pf/3. \tag{6.2}$$

Where f is a correlation term that allows for both the probability that the divalent cation which has just jumped from one site will immediately return to this site and the fact that a fraction of the jumps are perpendicular to the direction of diffusion, a_o is the cation-anion separation, ω_2 is the frequency with which the impurity makes a jump, and p is the degree of association. Writing ω_2 as a Boltzman expression

$$\omega_2 = \nu_2 \exp(-U_o/kT), \tag{6.3}$$

ν_2 is the frequency of vibration of the impurity in the lattice, and U_o is the activation energy barrier that the impurity ion must overcome in exchanging lattice sites. Also, p is temperature dependent and can be written as

$$p = \frac{[V_c^-]\ 12 \exp(-\Delta H/kT) \exp(\Delta S^1/k)}{1 + [V_c^-]\ 12 \exp(-\Delta H/kT) \exp(\Delta S^1/k)}, \tag{6.4}$$

where $(\Delta H - T\Delta S^1)$ has been substituted for the Gibbs free energy of association.

Using equations (6.3) and (6.4), D_T is now written as

$$D_T = \frac{D_o [V_c^-] \exp -(\Delta H + U_o)/kT \exp(\Delta S^1/k)}{1 + [V_c^-] 12 \exp(-\Delta H/kT) \exp(\Delta S^1/k)} , \qquad (6.5)$$

where the constant D_o is given by

$$D_o = 4 a_o^2 f \nu_2 . \qquad (6.6)$$

Therefore, if $12 [V_c^-] \exp(-\Delta H/kT) \exp(\Delta S^1/k) << 1$, the activation energy calculated form a plot of $\log_{10} D_T$ versus $1/T$ is the sum of the migration energy of the impurity and the enthalpy of the formation of the impurity-vacancy complex, and the migration energy can only be determined if the value of the enthalpy of formation is known. If $12 [V_c^-] \exp(-\Delta H\ kT) \exp(\Delta S^1/k) >> 1$, the activation energy calculated is the migration energy of the impurity. Because of these two limiting conditions, it is obvious that any activation energy estimated from a plot of $\log_{10} D_T$ versus $1/T$, when the concentration dependence of D_T has not been taken into account, must be critically analyzed as to what it represents. The situation is further complicated if the cation vacancies have been produced thermally, rather than by doping. Thus, if the Gibbs free energies of association are not accurate, the activation energy measured may not be

correct.

The activation energies measured in this work are the migration energies of the divalent cation since the Gibbs free energy of association has been considered in the calculation of D_s. Table (6.2) shows a comparison of activation energies with the ionic radii of various cations. Only studies in which the activation energy should represent the migration energy are included. The most obvious deviation in the values of the activation energies is that of Pb^{++} in KCl. In this case, U_o is measured as 1.18 ev by Keneshea et al. (22) and as 0.91 ev in this work. Possible explanations of interactions in impure host crystals which could lead to this deviation have already been presented. The value of 0.91 ev is a more reasonable value when the migration energies of Pb^{++} in KCl and NaCl are compared. That a smaller cation should have a lower migration energy in the same lattice, or that the same cation should have a lower migration energy in the more open lattice of KCl seems reasonable, and this is the general trend except for the results of Mannion (27, p. 62, 77-82) and Keneshea et al.

Bassani and Fumi (4) have calculated theoretical binding energies for complexes with Cd^{++}, Ca^{++}, and Sr^{++} in both KCl and NaCl. Two generalizations noted in their work were that the binding energy increased with the radius of the divalent cation, and that it also increased for the same ion when going from KCl to NaCl. The

Table 6.2. Values of the migration energy U_o for impurity ions in NaCl and KCl.

Crystal	Cation	Radius[a] (A)	U_o (ev)	Reference
NaCl	Pb^{++}	1.21	0.98[b]	28
			0.99[c]	3
			0.98[c]	This work
NaCl	Cd^{++}	0.97	0.92[b]	2
			0.86[c]	This work
NaCl	Mn^{++}	0.80	0.89[c]	27, p. 62
NaCl	Na^{+}	0.95		
KCl	Pb^{++}	1.21	1.18[b]	23
			0.91[c]	This work
KCl	Hg^{++}	1.10	0.57[c]	1, p. 117
KCl	Cd^{++}	0.97	0.54[b]	20
			0.56[c]	This work
KCl	Mn^{++}	0.80	1.05[c]	27, p. 77-82

a. Ionic radii from Pauling (30, p. 505-562).
b. Harshaw crystals.
c. Crystals grown from ion-exchange purified salt.

first of these generalizations are in complete disagreement with the results of this work if the pressure-volume work in forming the complex is considered small, as then the binding energy should approximately be the negative of the enthalpy of formation. Results of work by Rothman et al. (32) and of the works listed in Table (6.2) are also in conflict with this generalization. Bassani et al. used Pauling radii in their calculations and it has been found that Tosi-Fumi radii (15, 37) give better results for lattice calculations; however, the trends in the size of the radii are the same.

VII. SUMMARY

By a common ion treatment, the Stasiw-Teltow-Lidiard association theory was adapted to include the effect of two impurity ions on the equilibrium of the impurity-vacancy complex. A method of finite differences was adapted to solve two diffusion equations simultaneously when the diffusing species are the impurity-vacancy complexes.

Simultaneous diffusion of Pb^{++} and Cd^{++} in KCl crystals was studied. The saturation diffusion coefficient for the Pb^{++}-vacancy complex can be represented by

$$D_{s(Pb)} = 1.00 \times 10^{-3} \exp(-0.908 ev/kT) \text{ cm}^2/\text{sec} \qquad (7.1)$$

and that for the Cd^{++}-vacancy complex by

$$D_{s(Cd)} = 4.05 \times 10^{-5} \exp(-0.557 ev/kT) \text{ cm}^2/\text{sec}. \qquad (7.2)$$

The Gibbs free energy of association of the impurity-vacancy complex in KCl for lead can be represented as

$$\Delta G_{Pb} = -0.378 ev - (1.604 \times 10^{-4} ev/°K)\ T \qquad (7.3)$$

and for cadmium as

$$\Delta G_{Cd} = -0.474 ev - (1.230 \times 10^{-4} ev/°K)\ T\ . \qquad (7.4)$$

Simultaneous diffusion of Pb^{++} and Cd^{++} in NaCl crystals was also studied. The saturation diffusion coefficient for the Pb^{++}-vacancy complex can be represented by

$$D_{s(Pb)} = 1.40 \times 10^{-2} \exp(-0.982 ev/kT) \text{ cm}^2/\text{sec} \qquad (7.5)$$

and that for the Cd^{++}-vacancy complex by

$$D_{s(Cd)} = 3.57 \times 10^{-3} \exp(-0.857 ev/kT) \text{ cm}^2/\text{sec}. \qquad (7.6)$$

The Gibbs free energy of association of the impurity-vacancy complex in NaCl for lead can be represented as

$$\Delta G_{Pb} = -0.775 ev + (5.29 \times 10^{-4} ev/°K)\ T \qquad (7.7)$$

and for cadmium as

$$\Delta G_{Cd} = -0.972 ev + (6.65 \times 10^{-4} ev/°K)\ T. \qquad (7.8)$$

BIBLIOGRAPHY

1. Allen, C. A. Diffusion, conductivity and spectral properties of mercury II ion in potassium chloride crystals. Ph. D. thesis. Corvallis, Oregon State University, 1969. 141 numb. leaves.

2. Allen, C. A., D. T. Ireland and W. J. Fredericks. Diffusion of Cd^{+2} ions in single-crystal sodium chloride. Journal of Chemical Physics 47:3068-3072. 1967.

3. _____ Diffusion of lead ions in sodium chloride. Journal of Chemical Physics 46:2000-2001. 1967.

4. Bassani, F. and F. G. Fumi. The interaction between equilibrium defects in the alkali halides: the "ground state" binding energies between divalent impurities and vacancies. Il Nuovo Cimento 11:274-284. 1954.

5. Brand. Neues Jahrbuch fur Mineralogie, Geologie and Palaontologie, Beilage Band 32:627. 1911. (Cited In: National Research Council of the USA. International critical tables of numerical data, physics, chemistry and technology. Vol. 4. New York, McGraw-Hill, 1928. p. 55)

6. Carslaw, H. S. and J. C. Jaeger. Conduction of heat in solids. 2d ed. London, Oxford University, 1959. 510 p.

7. Chapman, Alan J. Heat transfer. 2d ed. New York, Macmillan, 1967. 617 p.

8. Crank, J. The mathematics of diffusion. London, Oxford University, 1964. 325 p.

9. Dreyfus, R. W. and A. S. Nowick. Energy and entropy of formation and motion of vacancies in NaCl and KCl crystals. Journal of Applied Physics, vol. 33, sup., p. 473-477. 1962.

10. Dusinberre, George Merrick. Heat-transfer calculations by finite differences. Scranton, International Textbook, 1961. 293 p.

11. Fredericks, W. J., F. E. Rostoczy and J. Hatchett. Investigation of crystal growth processes. Palo Alto, 1963. 24 numb. leaves. (Stanford Research Institute. Final report on SRI Project #PAU-3523)

12. Fredericks, W. J., L. W. Schuerman and L. C. Lewis. An investigation of crystal growth processes. Corvallis, 1966. 78 numb. leaves. (Oregon State University. Dept. of Chemistry. Final reports on Air Force Contracts AF-AFOSR-217-73 and AF-AFOSR-217-66)

13. Fritz, Bernd, Fritz Lüty and Jörg Anger. Der Einfluss von OH^--Ionen auf Absorptionsspektrum und Ionenleitfähigkeit KCl-Einkristallen. Zeitschrift fur Physik 174:240-256. 1963.

14. Fuller, Robert G. The chloride ion diffusion in potassium chloride. Ph.D. thesis. Urbana, University of Illinois, 1965. 72 numb. leaves.

15. Fumi, F. G. and M. P. Tosi. Ionic sizes and Born repulsive parameters in the NaCl-type alkali halides. I. The Huggins-Mayer and Pauling forms. Journal of Physical Chemistry of Solids 25:31-43. 1964.

16. Gie, T. I. and M. V. Klein. Infrared and ultra violet OH bands in hydroxide-doped KCl, KBr, NaCl and NaBr. Bulletin of the American Physical Society 8:230. 1963.

17. Girifalco, L. A. Atomic migration in crystals. New York, Academic, 1964. 162 p.

18. Howard, R. E. and A. B. Lidiard. Matter transport in solids. Report on Progress in Physics 27:161-240. 1964.

19. Jost, W. Diffusion in solids, liquids, gases. New York, Academic, 1952. 558 p.

20. Keneshea, F. J. and W. J. Fredericks. Diffusion of cadmium ions in solid potassium chloride. Journal of Physics and Chemistry of Solids 26:501-508. 1965.

21. _____ The diffusion of lead ions in potassium chloride. Palo Alto. 1962. 33 numb. leaves. (Stanford Research Institute. Report on Contract no. 19(604)-7231, project 5621, task 562001)

22. Keneshea, F. J. and W. J. Fredericks. Diffusion of lead ions in potassium chloride. Journal of Chemical Physics 38:1952-1958. 1963.

23. _____ Diffusion of lead ions in potassium chloride. Journal of Chemical Physics 41:3271-3272. 1964.

24. _____ On the diffusion parameters of plumbous ions in KCl. Journal of Chemical Physics 43:2925. 1965.

25. Lidiard, A. B. Ionic conductivity. Handbuch der Physik 20: 246-349. 1957.

26. _____ Ionic conductivity of impure polar crystals. Physical Review 94:29-37. 1954.

27. Mannion, W. A. A study of the Mn^{+2} and Pb^{+2}-Mn^{+2} impurity systems in alkali chlorides. Ph.D. thesis. Corvallis, Oregon State University, 1969. 144 numb. leaves.

28. Mannion, W. A., C. A. Allen and W. J. Fredericks. Diffusion of lead ions in purified NaCl crystals. Journal of Chemical Physics 48:1537-1540. 1968.

29. Matano, Chujiro. On the relation between the diffusion-coefficients and concentration of solid metals (the nickel-copper system). Japanese Journal of Physics 8:109-113. 1933.

30. Pauling, Linus. The nature of the chemical bond. 3d ed. Ithica, Cornell University, 1960. 644 p.

31. Reisfeld, R., A. Glasner and A. Honigbaum. On the diffusion parameters of plumbous ions in KCl. Journal of Chemical Physics 43:2923-2925. 1965.

32. Rothman, S. J. et al. Diffusion and conductivity in the NaCl-$ZnCl_2$ system. Philosophical Magazine, ser. 8. 14:501-513. 1963.

33. Schmidt, E. Föppls Festschrift. Springer, 1924. 179 p. (Cited in: Crank, J. The mathematics of diffusion. London, Oxford University, 1964. p. 187)

34. Schuerman, L. Unpublished research on chemical analysis of KCl and NaCl purified by ion-exchange. Corvallis, Oregon State University, Dept. of Chemistry, 1968. 1 numb. leave.

35. Shewmon, Paul G. Diffusion in solids. New York, McGraw-Hill, 1963. 203 p.

36. Stasiw, O. and J. Teltow. Über Fehlordnungserscheinungen in Silberhalogegeiden mit Zusatzen. Annales für Physik 1:261-272. 1947.

37. Tosi, M. P. and F. G. Fumi. Ionic sizes and Born repulsive parameters in the NaCl-type alkali halides. II. The generalized Huggins-Mayer form. Journal of Physics and Chemistry of Solids 25:45-57. 1964.

38. Watkins, G. D. Electron spin resonance of Mn^{+2} in alkali chlorides: association with vacancies and impurities. Physical Review 113:79-90. 1959.

APPENDIX

APPENDIX I

Raw data for diffusion experiments. A^1 has units of counts/min.

KCl 367°C $t_t = 1.6640 \times 10^6$ sec.

For $CdCl_2$ $C_c = 1.24$ mg/ml, $V_c = 0.500$ ml $V_t = 4.00$ ml

For $PbCl_2$ $C_c = 1.00$ mg/ml, $V_c = 0.500$ ml $V_t = 2.00$ ml

Crystal A Area = 1.2857 cm^2

	ω (mg)	A^1_{68kev}	A^1_{86kev}		A^1_{46kev}	A^1_{86kev}
1.	7.678	9624	522	Sep	252	108
2.	7.993	7991	451	Sep	230	105
3.	8.189	5894	381	Sep	169	102
4.	7.383	4140	298	Sep	158	103
5.	8.895	3342	276	Sep	151	115
6.	7.426	1739	200	Sep	77	102
7.	7.332	1023	164	Sep	64	103
8.	7.558	553	144	Sep	49	118
9.	7.572	260	137	Sep	50	120
10.	7.505	104	131	Sep	39	120
11.	12.120	68	186	Sep	47	171
12.	12.007	54	158	Sep	45	152
13.	12.081	51	152	Sep	50	148
14.	15.142	47	159	Sep	56	152
15.	15.192	51	139			
16.	15.403	50	114			
17.	15.046	44	95			
18.	15.122	43	73			
	Crystal B	Area = 1.2976 cm^2				
1.	7.325	8826	501	Sep	229	117
2.	9.981	9999	586	Sep	269	125
3.	10.844	7664	501	Sep	196	135
4.	10.411	4481	360	Sep	114	130
5.	10.658	2586	270	Sep	94	139
6.	10.875	1191	215	Sep	69	147
7.	10.695	427	188	Sep	56	164
8.	10.760	141	176	Sep	49	142

	ω (mg)	A^1_{46kev}	A^1_{86kev}		A^1_{46kev}	A^1_{86kev}
9.	10.684	63	173	Sep	44	164
10.	10.377	53	161	Sep	47	167
11.	12.250	51	160	Sep	48	145
12.	12.242	49	146	Sep	45	131
13.	12.300	50	132	Sep	40	125
14.	15.358	47	137	Sep	53	124
15.	15.344	46	112			
16.	13.628	41	98			
17.	15.322	40	75			
18.	15.288	39	57			
Background		38	33		40	39
Pb	0.050 ml	60,121	3142		59,200	3151
Pb	0.025 ml	30,090	1587		29,580	1611
Cd	0.050 ml	1,190	15,565		1,113	15,087
Cd	0.025 ml	575	7835		535	7481

KCl 455°C $t_t = 3.9200 \times 10^5$ sec.

For $CdCl_2$ $C_c = 1.24$ mg/ml $V_c = 0.500$ ml, $V_t = 4.00$ ml

For $PbCl_2$ $C_c = 1.00$ mg/ml $V_c = 0.500$ ml, $V_t = 2.00$ ml

Crystal A Area = 0.6436 cm^2

	ω (mg)	A^1_{46kev}	A^1_{86kev}		A^1_{46kev}	A^1_{86kev}
1.	3.496	8751	651	Sep	1009	320
2.	4.584	10307	130	Sep	699	314
3.	3.870	7098	510	Sep	784	285
4.	3.774	5599	498	Sep	474	257
5.	5.024	5809	592	Sep	562	335
6.	5.012	4070	521	Sep	459	319
7.	4.983	2633	489	Sep	210	313
8.	5.182	1572	465	Sep	245	326
9.	5.953	818	503	Sep	122	390
10.	5.164	322	410	Sep	84	332
11.	6.396	152	477	Sep	60	382
12.	6.431	86	421	Sep	64	344
13.	6.459	62	367	Sep	81	368
14.	6.384	60	324			
15.	6.429	55	279			
16.	6.285	70	342			

	ω (mg)	A^1_{46kev}	A^1_{86kev}		A^1_{46kev}	A^1_{86kev}
17.	6.421	53	193			
18.	6.476	47	157			
19.	6.513	43	121			
20.	6.420		90			
21.	6.823		65			
22.	6.493		43			
23.	6.437		37			
Crystal B - desorption at 450°C				Area = 0.6808 cm^2		
1.	4.650	6015	385			
2.	4.232	5724	361	Sep	361	165
3.	3.942	5425	349	Sep	346	153
4.	3.974	5163	341	Sep	352	160
5.	5.170	5862	434	Sep	634	219
6.	5.308	4587	406	Sep	490	223
7.	5.288	3236	392	Sep	272	220
8.	5.387	2108	385	Sep	221	258
9.	5.010	1146	348	Sep	111	259
10.	5.352	675	368	Sep	96	278
11.	5.386	316	378	Sep	78	285
12.	5.434	170	365	Sep	56	302
13.	5.313	92	340	Sep	62	288
14.	6.415	74	375	Sep	69	296
15.	6.819	78	362	$t_t = 8.920 \times 10^4$ sec.		
16.	6.731	79	299			
17.	6.658	58	283			
18.	10.086	64	329			
19.	7.939	52	214			
20.	6.710		156			
21.	6.700		124			
22.	6.612		96			
Background		39	36		37	32
Ph	0.050 ml	60976	3153		59750	3097
Pb	0.025 ml	30581	1621		30050	1585
Cd	0.050 ml	1416	18368		1091	15187
Cd	0.025 ml	687	9266		528	7609

KCl 458°C $t_t = 8.336 \times 10^4$ sec.

For $CdCl_2$ $C_c = 1.24$ mg/ml $V_c = 0.500$ ml $V_t = 4.00$ ml

For $PbCl_2$ $C_c = 1.00$ mg/ml $V_c = 0.500$ ml $V_t = 2.00$ ml

Crystal A Area = 0.7351 cm^2 Crystal B Area = 0.7351 cm^2

	ω (mg)	A^1_{46kev}	A^1_{86kev}	ω (mg)	A^1_{46kev}	A^1_{86kev}
1.	2.184	12285	4789	4.373	17905	2659
2.	4.180	16717	1947	4.721	12314	1550
3.	3.814	9143	1278	3.860	5812	1013
4.	4.556	4892	1011	3.991	2926	816
5.	4.517	2419	932	4.235	1648	832
6.	4.456	857	857	4.051	570	750
7.	4.238	257	772	4.153	219	667
8.	4.240	109	679	4.255	110	608
9.	4.304	90	593	4.206	87	532
10.	3.927	78	474	4.195	64	444
11.	5.676		554	4.772		463
12.	5.558		399	5.617		339
13.	5.718		306	5.982		233
14.	5.825		202	5.666		146
15.	7.166		111	6.962		77
16.	7.106		38	7.066		36
Background		38	36		38	36
Pb	0.050 ml	62787	3335		62787	3335
Pb	0.025 ml	31328	1686		31328	1686
Cd	0.050 ml	2260	26543		2260	26543
Cd	0.025 ml	1049	13159		1049	13159

KCl 492°C $t_t = 8.6800 \times 10^5$ sec.

For $CdCl_2$ $C_c = 1.24$ mg/ml $V_c = 0.500$ ml $V_t = 4.00$ ml

For $PbCl_2$ $C_c = 1.00$ mg/ml $V_c = 0.500$ ml $V_t = 2.00$ ml

Crystal A Area = 1.010 cm^2

	ω (mg)	A^1_{46kev}	A^1_{86kev}		A^1_{46kev}	A^1_{86kev}
1.	13.116	32415	2806	Sep	3029	1103
2.	5.688	10342	1039	Sep	944	475
3.	6.070	7453	929	Sep	663	485
4.	8.260	6505	1079	Sep	419	615
5.	7.814	3170	876	Sep	258	584
6.	7.796	1252	758	Sep	145	555

	ω (mg)	A^1_{46kev}	A^1_{86kev}		A^1_{46kev}	A^1_{86kev}
7.	7.874	398	656	Sep	93	510
8.	7.784	130	548	Sep	71	410
9.	7.778	82	436	Sep	60	344
10.	7.881	70	344	Sep	57	264
11.	7.803	59	255	Sep	54	192
12.	7.813	51	176	Sep	46	135
13.	8.051	48	114	Sep	58	94

Crystal B Area = 1.005 cm^2

1.	7.296	20492	1701	Sep	608	578
2.	12.962	25608	2481	Sep	407	973
3.	5.700	5977	860	Sep	224	433
4.	5.558	3730	735	Sep	148	433
5.	5.854	2006	692	Sep	97	466
6.	5.664	864	609	Sep	74	441
7.	5.699	331	557	Sep	63	431
8.	5.878	143	520	Sep	64	393
9.	5.688	100	426	Sep	50	335
10.	5.854	77	395	Sep	58	299
11.	5.813	64	339	Sep	51	246
12.	5.717	64	273	Sep	40	213
13.	5.748	53	209	Sep	43	163
14.	5.802	51	174	Sep	42	136
15.	5.783	51	135	For crystal B same Sep.		
16.	5.687	47	91	Standards as used for KCl		
17.	6.155	45	59	367°C Sep.		
				Standards for Crystal A Sep.		
Background		41	39		37	32
Pb	0.050 ml	60423	3209		60567	3306
Pb	0.025 ml	30441	1649		30270	1671
Cd	0.050 ml	1444	18917		1120	15187
Cd	0.025 ml	702	9482		570	7609

KCl 509° C $t_t = 7.292 \times 10^4$ sec

For $CdCl_2$ $C_c = 1.24$ mg/ml $V_c = 0.500$ ml $V_t = 4.00$ ml

For $PbCl_2$ $C_c = 1.00$ mg/ml $V_c = 0.500$ ml $V_t = 4.00$ ml

Crystal A Area = 0.6087 cm^2 Crystal B Area = 0.6176 cm^2

	ω (mg)	A^1_{46kev}	A^1_{86kev}	ω (mg)	A^1_{46kev}	A^1_{86kev}
1.	2.184	7524	1703	1.115	3894	811
2.	4.180	12229	2371	4.102	12650	2433

	ω (mg)	A^1_{46kev}	A^1_{86kev}	ω (mg)	A^1_{46kev}	A^1_{86kev}
3.	3.814	8983	1978	3.181	9074	1703
4.	4.556	7666	2129	3.588	7166	1796
5.	4.527	4670	1916	3.598	5141	1629
6.	4.456	2354	1690	3.593	3520	1530
7.	3.467	901	1261	3.494	1998	1397
8.	3.578	444	1221	3.475	1058	1312
9.	3.564	235	1125	3.468	496	1230
10.	3.592	149	1021	3.572	251	1163
11.	4.791	139	1166	4.679	180	1359
12.	4.752	105	978	4.773	137	1169
13.	4.738	100	795	4.761	107	943
14.	4.921	91	662	4.692	93	786
15.	5.924	89	588	5.899	97	758
16.	5.970	72	395	5.920	76	530
17.	6.013	55	216	6.022	68	335
18.	6.012	47	82	7.165	73	171
Background		42	38		42	38
Pb	0.050 ml	27640	1535		27640	1535
Pb	0.050 ml	28045	1550		28045	1550
Cd	0.050 ml	2378	26756		2378	26756
Cd	0.025 ml	1117	13398		1117	13398

KCl 553°C $t_t = 7.716 \times 10^4$ sec.

For $CdCl_2$ $C_c = 1.24$ mg/ml, $V_c = 0.500$ ml, $V_t = 4.00$ ml

For $PbCl_2$ $C_c = 1.00$ mg/ml, $V_c = 0.500$ ml, $V_t = 2.00$ ml

Crystal A Area = 0.5433 cm^2

	ω (mg)	A^1_{46kev}	A^1_{86kev}
1.	4.128	19588	1643
2.	4.476	16124	1503
3.	3.907	12651	1209
4.	4.241	9883	1116
5.	4.252	7311	1039
6.	4.676	5009	994
7.	4.404	2919	896
8.	4.080	1329	767
9.	4.224	695	761
10.	4.191	278	681
11.	5.156	180	696
12.	5.403	144	600
13.	5.190	96	473
14.	5.177	74	370

	ω (mg)	A^1_{46kev}	A^1_{86kev}
15.	5.178	69	289
16.	5.350	55	208
17.	5.282	47	132
18.	5.597		64
19.	5.180		37
20.	5.259		31
Background		35	31
Pb	0.050 ml	57803	3072
Pb	0.025 ml	28986	1563
Cd	0.050 ml	16154	1361
Cd	0.025 ml	8260	702

NaCl 347°C $t_t = 1.1239 \times 10^5$ sec.

For $CdCl_2$ $C_c = 1.24$ mg/ml $V_c = 0.250$ ml $V_t = 4.00$ ml

For $PbCl_2$ $C_c = 1.00$ mg/ml $V_c = 0.250$ ml $V_t = 2.00$ ml

	Crystal A Area = 0.7600 cm^2			Crystal B Area = 0.6877 cm^2		
	ω (mg)	A^1_{46kev}	A^1_{86kev}	ω (mg)	A^1_{46kev}	A^1_{86kev}
1.	2.586	1318	2398	3.348	1707	5277
2.	5.192	2447	4329	3.753	1778	5807
3.	4.843	2017	3719	4.326	1848	6481
4.	4.835	1663	3476	4.432	1595	6072
5.	3.643	1051	2432	3.990	1197	5131
6.	5.151	1209	3110	4.390	1073	5233
7.	4.704	810	2516	4.366	793	4755
8.	4.884	578	2311	4.011	542	3940
9.	4.804	390	2002	4.318	424	3830
10.	4.834	259	1779	4.367	298	3451
11.	4.423	147	1422	4.451	205	3087
12.	5.074	98	1394	4.316	139	2637
13.	5.013	57	1159	4.215	90	2240
14.	5.990	40	1115	4.436	64	2025
15.	3.994	18	597	4.458	45	1719
16.	5.023	16	604	4.338	33	1400
17.	5.002	13	480	4.307	24	1158
18.	4.610	17	384	4.006	20	906
19.	4.992	17	274	4.393	17	801
20.	4.591		184	4.304	8	620
21.	6.475		170	4.138		478
22.	6.494		96	4.523		407
23.	7.834		74	5.404		353

	ω (mg)	A^1_{46kev}	A^1_{86kev}	ω (mg)	A^1_{46kev}	A^1_{86kev}
24.	8.388		39	5.716		344
25.	7.878		31	7.592		198
26.				7.406		92
27.				7.340		48
Background		8	17			
Pb	0.050 ml	7974	762.5			
Cd	0.050 ml	299	14837	Same St. as A.		

NaCl 360°C $t_t = 1.2890 \times 10^6$ sec.

For $CdCl_2$ $C_c = 1.24$ mg/ml $V_c = 0.500$ ml $V_t = 4.00$ ml

For $PbCl_2$ $C_c = 1.00$ mg/ml $V_c = 0.500$ ml $V_t = 2.00$ ml

Crystal A Area = 1.7772 cm^2 Crystal B Area = 1.1707 cm^2

	ω (mg)	A^1_{46kev}	A^1_{86kev}	ω (mg)	A^1_{46kev}	A^1_{86kev}
1.	8.967	14951	6940	4.979	8480	3750
2.	13.020	16844	8768	10.224	14940	5629
3.	11.971	11944	7226	10.001	11544	4994
4.	12.079	8455	6413	10.031	8899	4488
5.	12.099	5740	5604	20.020	11039	7319
6.	12.047	3624	4769	9.970	2931	2967
7.	12.056	2117	4071	10.032	1860	2579
8.	11.987	1154	3369	10.032	1089	2166
9.	14.124	704	3174	10.038	622	1850
10.	14.156	349	2487	10.057	347	1546
11.	14.268	201	1884	13.987	246	1661
12.	13.932	132	1306	13.941	147	1195
13.	15.996	112	1003	14.039	99	838
14.	16.210	77	593	14.063	71	563
15.	16.078	61	308	17.990	66	399
16.	16.052	44	156	14.075	54	195
17.	20.160	45	70	18.099	42	82
18.	20.321	55	45	18.247	39	43
Background		43	40		43	40
Pb	0.050 ml	49291	3152		59291	3152
Pb	0.025 ml	29733	1487		29733	1587
Cd	0.050 ml	1101	14578		1101	14578
Cd	0.025 ml	545	7282		545	7282

NaCl 409° C $t_t = 2.451 \times 10^5$ sec.

For $CdCl_2$ $C_c = 1.24$ mg/ml, $V_c = 0.500$ ml, $V_t = 4.00$ ml

For $PbCl_2$ $C_c = 1.00$ mg/ml, $V_c = 0.500$ ml, $V_t = 2.00$ ml

	Crystal A Area = 0.7600 cm^2			Crystal B Area = 0.7600 cm^2		
	ω (mg)	A^1_{46kev}	A^1_{86kev}	ω (mg)	A^1_{46kev}	A^1_{86kev}
1.	5.106	11653	1392	2.865	5109	2504
2.	6.230	10209	1078	4.134	4063	1584
3.	6.897	8468	969	7.072	11559	4936
4.	5.250	4508	623	6.331	7649	3722
5.	5.226	3079	512	6.279	5353	3166
6.	5.224	1903	425	6.343	3287	2623
7.	5.289	1103	365	6.386	1897	2132
8.	5.255	531	288	6.335	936	1689
9.	5.265	214	229	6.320	416	1268
10.	5.262	88	160	6.368	192	976
11.	5.119	59	118	7.482	118	751
12.	5.304	48	77	7.824	78	447
13.	5.360	43	56	7.920	56	218
14.	6.423		42	7.940	42	86
15.	6.957		39	7.577	46	45
Background		40	35		40	35
Pb	0.050 ml	60241	3201		60241	3201
Pb	0.025 ml	31120	1603		31120	1603
Cd	0.050 ml	1183	15988		1183	15988
Cd	0.025 ml	569	7981		569	7981

NaCl 460°C $t_t = 1.674 \times 10^5$ sec.

For $CdCl_2$ $C_c = 1.24$ mg/ml $V_c = 0.500$ ml $V_t = 4.00$ ml

For $PbCl_2$ $C_c = 1.00$ mg/ml $V_c = 0.500$ ml $V_t = 2.00$ ml

	Crystal A Area = 0.5692 cm^2			Crystal B Area = 0.5753 cm^2		
	ω (mg)	A^1_{46kev}	A^1_{86kev}	ω (mg)	A^1_{46kev}	A^1_{86kev}
1.	2.016	8752	6127	5.746	25157	18059
2.	3.764	16701	11302	4.528	17361	13350
3.	3.522	13317	9840	3.635	11912	9909
4.	3.520	11637	9208	4.953	13061	12139
5.	4.519	12345	10596	5.237	10568	11421
6.	4.221	8997	8840	4.915	7352	9285
7.	4.695	7779	8706	4.929	5180	8157
8.	4.789	5654	7843	4.911	3537	7052
9.	4.553	3582	6259	4.866	2368	5940

	ω (mg)	A^1_{46kev}	A^1_{86kev}	ω (mg)	A^1_{46kev}	A^1_{86kev}
10.	4.676	2549	5676	4.777	1410	4863
11.	4.800	1600	4849	6.085	1014	4968
12.	4.657	958	3882	6.164	596	3898
13.	4.751	672	3349	6.228	320	2842
14.	4.790	347	2610	6.126	189	1939
15.	5.950	265	2454	6.112	133	1263
16.	5.961	166	1682	5.900	89	714
17.	5.860		1052	6.209		391
18.	5.934		606			
19.	8.349		304			
20.	8.320		88			
Background		41	43		41	43
Pb	0.050 ml	61000	3239		61000	3239
Pb	0.025 ml	30581	1642		30581	1642
Cd	0.050 ml	1495	19502		1495	19502
Cd	0.025 ml	722	9648		722	9648

NaCl 497°C $t_t = 6.730 \times 10^4$ sec.

For $CdCl_2$ $C_c = 1.24$ mg/ml $V_c = 0.500$ ml $V_t = 4.00$ ml

For $PbCl_2$ $C_c = 1.00$ mg/ml $V_c = 0.500$ ml $V_t = 4.00$ ml

Crystal A Area = 0.8245 cm^2 Crystal B Area = 0.8598 cm^2

	ω (mg)	A^1_{46kev}	A^1_{86kev}	ω (mg)	A^1_{46kev}	A^1_{86kev}
1.	9.158	39371	56497	10.183	42736	61730
2.	6.242	22371	33899	6.381	22173	35336
3.	5.242	15432	26667	5.166	15037	26316
4.	5.182	12239	24096	5.614	13458	25773
5.	5.150	9625	21551	5.635	10741	22936
6.	5.262	7570	19920	5.643	8244	20284
7.	5.020	5192	16778	5.555	5963	17421
8.	5.189	3957	15197	5.504	4108	14749
9.	5.270	2878	13642	5.591	2990	12771
10.	5.311	1997	11467	5.507	2005	10504
11.	6.738	1623	11876	7.329	1662	11111
12.	7.037	684	9891	7.351	921	8237
13.	6.935	662	7225	7.396	552	5817
14.	6.849	434	5176	7.447	321	3751
15.	6.891	292	3600	7.381	186	2128
16.	6.689	191	2313	7.388	111	1048
17.	8.740	37	1655	9.256	37	482
18.	8.431	37	690	9.290	37	141
19.	8.679	38	205			

	ω (mg)	A^1_{46kev}	A^1_{86kev}	ω (mg)	A^1_{46kev}	A^1_{86kev}
Background		37	38		37	38
Pb	0.050 ml	28000	1525		28000	1525
Cd	0.050 ml	2200	29300		2200	29300

NaCl 502°C $t_t = 7.200 \times 10^4$ sec.

For $CdCl_2$ $C_c = 1.24$ mg/ml $V_c = 0.250$ ml $V_t = 4.00$ ml

For $PbCl_2$ $C_c = 1.00$ mg/ml $V_c = 0.750$ ml $V_t = 6.00$ ml

Crystal A Area = 0.4964 cm^2 Crystal B Area = 0.5484 cm^2

	ω (mg)	A^1_{46kev}	A^1_{86kev}	ω (mg)	A^1_{46kev}	A^1_{86kev}
1.	0.916	1792	1929	1.607	3871	3948
2.	3.849	11520	9328	3.876	11481	9643
3.	3.129	8673	7435	3.374	9337	8244
4.	3.126	7968	7168	3.417	8673	7994
5.	2.623	6017	5692	3.474	7728	7722
6.	3.240	6545	6745	3.352	6583	7117
7.	3.208	5429	6188	3.414	5672	6940
8.	3.693	4423	5770	3.622	4982	6873
9.	3.234	3546	5414	3.419	3752	6146
10.	3.107	2560	4753	3.258	2656	5268
11.	3.096	1872	4327	3.625	2119	5211
12.	3.102	1308	3923	3.537	1464	4666
13.	3.129	857	3489	3.405	898	3971
14.	3.322	550	3235	3.488	574	3608
15.	3.151	293	2636	3.279	311	2859
16.	3.298	166	2296	3.603	189	2699
17.	2.997	87	1787	3.341	96	2004
18.	3.078	57	1480	3.254	57	1559
19.	3.175	34	1055	3.611	39	1302
20.	3.214	28	742	3.166	23	825
21.	2.975	16	588	3.254	19	586
22.	4.419	10	367	3.235		359
23.	4.239		139	4.734		263
24.	4.421		57	4.852		99
25.	4.245		18	4.642		42
26.				4.892		32
Background		9	22		9	22
Pb	0.050 ml	8264	762		8264	762
Cd	0.050 ml	280	15337		280	15337

NaCl 553°C $t_t = 4.368 \times 10^4$ sec.

For $CdCl_2$ $C_c = 1.24$ mg/ml $V_c = 0.500$ ml $V_t = 4.00$ ml

For $PbCl_2$ $C_c = 1.00$ mg/ml $V_c = 0.500$ ml $V_t = 2.00$ ml

	Crystal A Area = 0.7991 cm^2			Crystal B Area = 0.4894 cm^2		
	ω (mg)	A^1_{46kev}	A^1_{86kev}	ω (mg)	A^1_{46kev}	A^1_{86kev}
1.	2.946	11649	4347	3.567	25597	9314
2.	5.518	43379	15027	4.287	32847	11501
3.	4.942	37369	13091	4.243	28063	10829
4.	5.040	34969	12867	4.216	24896	10243
5.	4.976	30827	12036	4.322	20675	9720
6.	5.056	27586	11517	4.239	15763	8619
7.	4.654	21925	10124	4.273	11947	7900
8.	4.956	19731	10151	4.205	8142	6849
9.	4.998	16411	9478	4.196	5363	5909
10.	4.860	12680	8461	4.204	3370	5111
11.	6.702	12892	10489	5.263	2274	5066
12.	6.747	8776	9189	5.245	1015	3829
13.	6.736	5285	7792	5.364	480	2840
14.	6.802	3089	6505	5.260	205	1761
15.	6.776	1598	5156	5.342	121	1009
16.	8.516	942	4808	5.258	69	472
17.	8.493	416	3204	5.163	62	192
18.	8.467	250	1985	6.093	51	92
19.	8.354	117	999	5.993	42	50
20.	8.440	300	571	5.988	41	42
21.	8.379	63	184	6.899	47	42
Background		37	33		37	33
Pb	0.050 ml	60240	3193		60240	3193
Pb	0.025 ml	30030	1621		30030	1621
Cd	0.050 ml	1192	16062		1192	16062
Cd	0.025 ml	584	8080		584	8080

NaCl 569°C $t_t = 4.212 \times 10^4$ sec.

For $CdCl_2$ $C_c = 1.24$ mg/ml $V_c = 0.500$ ml $V_t = 8.00$ ml

For $PbCl_2$ $C_c = 1.00$ mg/ml $V_c = 1.00$ ml $V_t = 8.00$ ml

Crystal A Area = 0.4668 cm^2

	ω (mg)	A^1_{46kev}	A^1_{86kev}
1.	3.457	9403	1180
2.	3.108	9341	10680
3.	2.767	7748	9048

	ω (mg)	A^1_{46kev}	A^1_{86kev}
4.	2.830	7587	9026
5.	2.844	7184	8812
6.	2.916	6580	8424
7.	2.919	5969	8128
8.	2.869	4945	7494
9.	2.879	4388	7156
10.	2.965	3672	6824
11.	2.908	2935	6194
12.	2.904	2270	5726
13.	2.938	1717	5248
14.	2.954	1261	4768
15.	2.908	854	4226
16.	2.884	574	3656
17.	2.937	352	3128
18.	2.870	212	2542
19.	2.925	127	2182
20.	2.907	84	1755
21.	3.943	86	1684
22.	3.954	37	1062
23.	3.943	21	593
24.	4.864	15	306
25.	5.022		117
26.	4.946		34
27.	4.958		25
28.	4.941		21
Background		10	19
Pb	0.050 ml	7359	276
Cd	0.050 ml	12650	730